Effects of thermal expansion on moderately intense turbulence in premixed flames

Accepted to Phys. Fluids 10.1063/5.0123211

Effects of thermal expansion on moderately intense turbulence in premixed flames

Vladimir A. Sabelnikov[a,b], Andrei N. Lipatnikov[c,*], Nikolay V. Nikitin[d], Francisco E. Hernández-Pérez[e], Hong G. Im[e]

[a]*ONERA – The French Aerospace Laboratory, F-91761 Palaiseau, France*
[b]*Central Aerohydrodynamic Institute (TsAGI), 140180 Zhukovsky, Moscow Region, Russian Federation*
[c]*Department of Mechanics and Maritime Sciences, Chalmers University of Technology, Gothenburg, 41296 Sweden*
[d]*Lomonosov Moscow State University, Moscow, Russian Federation*
[e]*Clean Combustion Research Center, King Abdullah University of Science and Technology, Thuwal 23955-6900, Saudi Arabia*
**Corresponding author, lipatn@chalmers.se*

Abstract

The study aims at analytically and numerically exploring the influence of combustion-induced thermal expansion on turbulence in premixed flames. In the theoretical part, contributions of solenoidal and potential velocity fluctuations to the unclosed component of the advection term in the Reynolds-averaged Navier-Stokes equations are compared and a new criterion for assessing the importance of the thermal expansion effects is introduced. The criterion highlights a ratio of the dilatation in the laminar flame to the large-scale gradient of root-mean-square (rms) velocity in the turbulent flame brush. To support the theoretical study, direct numerical simulation (DNS) data obtained earlier from two complex-chemistry, lean H_2-air flames are analyzed. In line with the new criterion, even at sufficiently high Karlovitz numbers, results show significant influence of combustion-induced potential velocity fluctuations on the second moments of the turbulent velocity upstream of and within the flame brush. In particular, the DNS data demonstrate that (i) potential and solenoidal rms velocities are comparable in the unburnt gas close to the leading edge of the flame brush and (ii) potential and solenoidal rms velocities conditioned to unburnt gas are comparable within the entire flame brush. Moreover, combustion-induced thermal expansion affects not only the potential velocity, but even the solenoidal one. The latter effects manifest themselves in a negative correlation between solenoidal velocity fluctuations and dilatation or in the counter-gradient behavior of the solenoidal scalar flux. Finally, a turbulence-in-premixed-flame diagram is sketched to discuss the influence of combustion-induced thermal expansion on various ranges of turbulence spectrum.

Accepted to Phys. Fluids 10.1063/5.0123211

I. INTRODUCTION

Since the pioneering work by Karlovitz et al.[1] and Libby and Bray,[2] effects of thermal expansion on turbulence (e.g., so-called flame-generated turbulence[1]) and turbulent scalar transport (e.g., so-called counter-gradient diffusion[2]) in premixed flames have long been a challenging research subject.[3-15] Numerical studies reviewed elsewhere[16-19] indicate that the influence of combustion-induced thermal expansion on turbulence within a premixed flame brush is well (hardly) pronounced in weakly (highly) turbulent flames. Recent Direct Numerical Simulation[11,20-23] (DNS) and experimental[24,25] investigations further support this view. However, criteria for finding domains of importance of such an influence have not yet been well established.

One of the widely accepted criteria of this kind was suggested by Bray[26] who considered turbulent scalar transport to be counter-gradient if

$$N_B = \frac{(\sigma-1)S_L}{2\alpha u'} > 1. \quad (1)$$

Here, $\sigma = \rho_u/\rho_b$ is the density ratio; S_L is the laminar flame speed; u' is root-mean-square (rms) turbulent velocity; subscript u or b designates unburnt or burnt mixture, respectively; and the number N_B is known as Bray number. The factor α is of unity order and is expected to increase with increasing a ratio of an integral length scale L of turbulence to the laminar flame thickness δ_L.[27] Since a widely accepted model of α has not yet been developed, this factor is often omitted in Eq. (1). In any case, turbulent scalar transport is not the major subject of the present study, which is rather focused on the influence of combustion-induced thermal expansion on the second moments of the turbulent velocity field.

By considering the influence of combustion-induced thermal expansion on small-scale turbulent eddies, Bilger[28] has hypothesized that such an influence is significant if the magnitude τ_K^{-1} of velocity gradients in the smallest eddies is less than dilation $\Theta = (\sigma - 1)\tau_f^{-1}$ in the laminar flame. Therefore, the following criterion should hold

$$Ka < Ka_{cr}^{B} = \sigma - 1 \tag{2}$$

in order for the influence of combustion-induced thermal expansion on small-scale turbulent eddies to be substantial. Here, $Ka = \tau_f/\tau_K$ designates Karlovitz number; $\tau_f = \delta_L/S_L$ and $\tau_K = \eta_K/u_K = (\nu_u/\bar{\varepsilon})^{1/2}$ are the laminar flame and Kolmogorov time scales, respectively; $u_K = (\nu_u\bar{\varepsilon})^{1/4}$ and $\eta_K = (\nu_u^3/\bar{\varepsilon})^{1/4}$ are Kolmogorov velocity and length scales[25], respectively; ν is the kinematic viscosity of unburnt mixture; $\bar{\varepsilon} = 2\overline{\nu S_{jk}S_{jk}}$ is a mean dissipation rate; $S_{jk} = 0.5\left(\partial u_j/\partial x_k + \partial u_k/\partial x_j\right)$ is the rate-of-strain tensor; and summation convention applies to repeated indices. Note that (i) under conditions of a low Mach number, as in the case under study, dilatational contribution to the mean dissipation rate is commonly neglected if turbulence characteristics in Ka are evaluated in the incompressible flow of unburnt reactants; and (ii) to properly characterize the dilatation magnitude, the laminar flame thickness should be evaluated as follows: $\delta_L = (T_b - T_u)/\max|\nabla T|$, where T is the temperature. The simple criterion given by Eq. (2) was recently supported in a DNS study[30,31] of two stoichiometric H_2-air jet turbulent flames characterized by $Ka = 3.7 < Ka_{cr}^{B} = 6.7$ and $Ka = 54 > Ka_{cr}^{B}$.

Besides the influence of combustion-induced thermal expansion on the smallest turbulent eddies, addressed by Bilger,[28] larger eddies from the inertial range of Kolmogorov turbulence[29] may also be affected by the thermal expansion in flames.[10,32] In particular, O'Brien et al.[32] have theorized that thermal energy released by combustion and transformed

to kinetic energy at small scales can be transferred via inverse turbulence cascade to larger eddies (this phenomenon is known as backscatter) whose time scale is shorter than or equal to τ_f. MacArt and Mueller[10] have also argued that "competition between a heat-release-induced cascade and the classical, production-driven forward cascade" can appear under certain conditions even if $Ka > Ka_{cr}^{B}$.

As far as the largest turbulent eddies, whose length scale is on the order of L, are concerned, the present authors are not aware of a criterion characterizing the influence of combustion-induced thermal expansion on such eddies. This work aims primarily at bridging this knowledge gap.

In Sect. II, a new criterion is introduced by analyzing contributions of potential and solenoidal components of a fluctuating velocity field to various terms in transport equations for turbulent Reynolds stresses. To support this theoretical analysis, such potential and solenoidal contributions are explored by processing published DNS data described briefly in Sect. III. Results are reported in Sect. IV. The newly proposed criterion is compared with other relevant criteria in Sect. V, where a simple diagram is drawn to speculate what ranges of turbulence spectrum are substantially affected by combustion-induced thermal expansion in a premixed flame under various conditions. Conclusions are summarized in Sect. VI.

It is worth stressing that (i) the newly introduced criterion complements criteria suggested earlier, e.g., Eq. (2), rather than replacing them and (ii) another effect of combustion on turbulence, i.e., turbulence decay due to an increase in kinematic viscosity with the temperature, is not explored in the present paper, while this mechanism is considered in the DNS discussed in Sects. III and IV.

II. A THEORETICAL ANALYSIS

A. Reynolds-average framework

Let us consider the Reynolds-averaged Navier-Stokes equations written in a non-conservative form:

$$\frac{\partial \bar{u}_i}{\partial t} + \bar{u}_k \frac{\partial \bar{u}_i}{\partial x_k} + \overline{u_k' \frac{\partial u_i'}{\partial x_k}} = -\overline{\frac{1}{\rho}\frac{\partial p}{\partial x_\iota}} + \overline{\frac{1}{\rho}\frac{\partial \tau_{\iota k}}{\partial x_k}}. \tag{3}$$

Here, $u_i = \bar{u}_i + u_i'$ is i-th component of the velocity vector $\mathbf{u} = \bar{\mathbf{u}} + \mathbf{u}'$; t designates time; x_i are Cartesian coordinates; p is the pressure; τ_{ik} is the viscous stress tensor; and overbars designate Reynolds averages.

For constant-density flows, turbulence models aim at closing the Reynolds stresses $\overline{u_i' u_k'}$ or the last term on the left-hand side (LHS) of Eq. (3). Moreover, in constant-density turbulence in an unbounded domain, $\mathbf{u}'(\mathbf{x}, t)$ stems from a solenoidal (rotational) motion and $\nabla \cdot \mathbf{u}' = 0$. In flames, $\nabla \cdot \mathbf{u}' \neq 0$ due to thermal expansion, with combustion-induced pressure perturbations creating potential (irrotational) velocity fluctuations. Thus, eventual importance of combustion-induced thermal expansion effects could be assessed by comparing contributions of solenoidal and potential velocity fields to major turbulence characteristics. In the following, this task is pursued by examining the last term on the LHS of Eq. (3).

If one performs a Helmholtz-Hodge decomposition (HHD) of the velocity field $\mathbf{u}'(\mathbf{x}, t)$ into divergence-free solenoidal and irrotational potential fields, $\mathbf{u}_s'(\mathbf{x}, t)$ and $\mathbf{u}_p'(\mathbf{x}, t)$, respectively, the following equations hold[33]

$$u_i' = u_{s,i}' + u_{p,i}'; \quad \frac{\partial u_{s,k}'}{\partial x_k} = 0; \quad \frac{\partial u_{p,k}'}{\partial x_i} = \frac{\partial u_{p,i}'}{\partial x_k}. \tag{4}$$

The last equality results directly from $\nabla \times \mathbf{u}'_p = 0$. Substitution of Eqs. (4) into the last term on the LHS of Eq. (3) yields

$$\overline{u'_k \frac{\partial u'_\iota}{\partial x_k}} = \overline{u'_{s,k} \frac{\partial u'_{s,\iota}}{\partial x_k}} + \overline{u'_{s,k} \frac{\partial u'_{p,\iota}}{\partial x_k}} + \overline{u'_{p,k} \frac{\partial u'_{s,\iota}}{\partial x_k}} + \overline{u'_{p,k} \frac{\partial u'_{p,\iota}}{\partial x_k}}$$

$$= \frac{\partial \overline{u'_{s,\iota} u'_{s,k}}}{\partial x_k} + \frac{\partial \overline{u'_{p,\iota} u'_{s,k}}}{\partial x_k} + \frac{\partial \overline{u'_{p,k} u'_{s,\iota}}}{\partial x_k} - \overline{u'_{s,\iota} \frac{\partial u'_{p,k}}{\partial x_k}} + \overline{u'_{p,k} \frac{\partial u'_{p,k}}{\partial x_\iota}}$$

$$= \frac{\partial}{\partial x_k}\left(\overline{u'_{s,\iota} u'_{s,k}} + \overline{u'_{p,\iota} u'_{s,k}} + \overline{u'_{s,\iota} u'_{p,k}}\right) + \frac{1}{2}\frac{\partial}{\partial x_\iota}\overline{u'_{p,k} u'_{p,k}} - \overline{u'_{s,\iota} \frac{\partial u'_{p,k}}{\partial x_k}}. \quad (5)$$

The last term in the second line of Eq. (5) results from substitution of the last equality in Eq. (4) into the last term in the first line of Eq. (5).

In the simplest statistically one-dimensional (1D) and planar case, Eq. (5) reads

$$\overline{u'_k \frac{\partial u'_1}{\partial x_k}} = \underbrace{\frac{\partial \overline{u'^2_{s,1}}}{\partial x_1}}_{\dot{T}_1} + \underbrace{2\frac{\partial \overline{u'_{s,1} u'_{p,1}}}{\partial x_1}}_{\dot{T}_2} + \underbrace{\frac{1}{2}\frac{\partial \overline{u'_{p,k} u'_{p,k}}}{\partial x_1}}_{\dot{T}_3} - \underbrace{\overline{u'_{s,1} \frac{\partial u'_{p,k}}{\partial x_k}}}_{\dot{T}_4}. \quad (6)$$

Close to a boundary of importance of the studied thermal expansion effects, the order of magnitude of the potential velocity fluctuations cannot be larger than the order of magnitude of the rotational velocity fluctuations. Accordingly, within the mean flame brush, the order of magnitude of the first three terms on the right hand (RHS) of Eq. (6) is u'^2/δ_t or less. Here, δ_t is the mean flame brush thickness.

To estimate the order of magnitude of the last term, let us, first, similarly to Bilger,[28] assume that $\left|\nabla \cdot \mathbf{u}'_p\right|$ is on the order of $\Theta = (\sigma - 1)\tau_f^{-1}$. This assumption is in line with recent DNS and experimental data, which indicate that combustion is mainly localized to inherently laminar flamelets even at sufficiently high Ka, as reviewed elsewhere.[34,35] DNS data reported in Sect. IV support this assumption. It is also worth remembering that eventual decrease in

dilatation due to local flame broadening by small-scale turbulent eddies may be counterbalanced by (i) an increase in the dilatation magnitude due to straining of the local flame by larger turbulent eddies[36] and (ii) differential diffusion effects,[37] which are discussed in detail elsewhere.[38]

Second, to estimate the magnitude of the fourth term, let us also note that the correlation between solenoidal velocity fluctuations $\mathbf{u}_s'$ and dilatation $\nabla \cdot \mathbf{u}_p'$ does not vanish, because the vorticity transport equation involves a dilatation term.[16-19] This consideration will also be supported in Sect. IV.

Thus, the fourth term on the RHS of Eq. (6) is expected to be on the order of $u'\Theta = u'(\sigma - 1)\tau_f^{-1}$ bearing in mind that $\mathbf{u}_s'$ and $\mathbf{u}'$ are of the same order when the thermal expansion effects become relatively weak (close to the boundary we seek for). Therefore, the considered term, which involves potential velocity fluctuations, should play an important role unless the dilatation Θ is much smaller than u'/δ_t. Contrary to Eq. (2), this newly introduced criterion compares Θ with the large-scale gradient of the rms turbulent velocity in the mean flame brush, rather than with the small-scale velocity gradient in Kolmogorov eddies. As the former gradient is significantly smaller, the newly introduced criterion implies importance of thermal expansion effects in a wider domain of flame characteristics.

According to the new criterion, thermal expansion effects are of minor importance if the Damköhler number $Da = \tau_t/\tau_f$ is less than a critical value of

$$Da_{cr}^{-1} = (\sigma - 1)\frac{\delta_t}{L}, \tag{7}$$

where $\tau_t = L/u'$ is an integral time scale of turbulence.

The same criterion can be obtained in a different way. Let us consider the following well-known Reynolds-averaged transport equation[16-19,26,35]

$$\frac{\partial \bar{c}}{\partial t} + \overline{u_k \frac{\partial c}{\partial x_k}} = \overline{\frac{1}{\rho} \frac{\partial q_{c,k}}{\partial x_k}} + \overline{\frac{1}{\rho} \dot{\omega}_c} \tag{8}$$

for a combustion progress variable c, which characterizes mixture state in a flame and varies from zero in unburnt reactants to unity in the equilibrium adiabatic combustion products. Here, $q_{c,k}$ is k-th component of molecular flux $\mathbf{q}_c$ of c and $\dot{\omega}_c$ is the mass rate of product creation. The convection term, i.e., the second term on the LHS of Eq. (8), reads

$$\overline{u_k \frac{\partial c}{\partial x_k}} = \overline{\frac{\partial u_k c}{\partial x_k}} - \overline{c \frac{\partial u_k}{\partial x_k}} = \overline{\frac{\partial u_{s,k} c}{\partial x_k}} + \overline{\frac{\partial u_{p,k} c}{\partial x_k}} - \overline{c \frac{\partial u_{p,k}}{\partial x_k}}. \tag{9}$$

For the reasons presented above, within the mean flame brush, the order of magnitude of the first two terms on the RHS of Eq. (9) is u'/δ_t or less, whereas the order of magnitude of the third term is Θ. Thus, we arrive at Eq. (7) again.

In Eq. (7), the thickness δ_t is unknown *a priori*. Various experimental[39-42] and DNS[34,43-45] data show that $\delta_t/L > 1$. Therefore, Da_{cr} should be less than $(\sigma-1)^{-1} = O(10^{-1})$. Moreover, DNS data[43,44] indicate that mean thickness of a fully-developed turbulent premixed flame, i.e., a turbulent premixed flame propagating at a constant speed and having a constant thickness, scales as $\delta_{t,\infty}/L \propto (u'/S_L)^{1/3}$ in moderately intense ($u'/S_L \leq 10$, $Da > 0.2$) turbulence, whereas a subsequent DNS study[34] has yielded $\delta_{t,\infty}/L \propto Da^{-1/2}$ at $Da < 0.1$. Here, the subscript ∞ refers to the fully-developed flame. Let us invoke the latter scaling for δ_t/L, because Eq. (7) implies that a small $Da < O(10^{-1})$ is required for the thermal expansion effects to be of minor importance in turbulent flames. We arrive at

$$Da_{cr} = (\sigma-1)^{-2} \tag{10}$$

by disregarding numerical factors of unity order.

In the following the thickness $\delta_t = (T_b - T_u)/\max|\nabla \bar{T}|$ will be extracted from the DNS data.

B. Favre-average framework

In the combustion literature, Favre averaging is often used to reduce the number of unclosed terms in the Favre-averaged transport equations when compared to the Reynolds-averaged ones. Therefore, it is worth comparing contributions of potential and solenoidal velocities to the Favre-averaged second moments $\overline{\rho u_i'' u_k''}$. Here, $u_i'' \equiv u_i - \tilde{u}_i$ and $\tilde{u}_i \equiv \overline{\rho u_i}/\bar{\rho}$. However, defining Favre-averaged fluctuating solenoidal and potential velocity fields is not trivial. Indeed, because

$$u_i'' = u_i - \tilde{u}_i = \bar{u}_i + u_i' - \tilde{u}_i = \bar{u}_i + u_i' - \frac{\overline{\rho u_i}}{\bar{\rho}}$$

$$= \bar{u}_i + u_i' - \frac{\overline{\rho \bar{u}_i}}{\bar{\rho}} - \frac{\overline{\rho u_i'}}{\bar{\rho}} = u_i' - \frac{\overline{\rho u_i'}}{\bar{\rho}} = u_i' - \widetilde{u_i'}, \tag{11}$$

the fields $\mathbf{u}'(\mathbf{x}, t)$ and $\mathbf{u}''(\mathbf{x}, t)$ cannot be divergence-free (or irrotational) simultaneously. Since $\mathbf{u}'(\mathbf{x}, t)$ directly characterizes the fluctuating velocity field, whereas $\mathbf{u}''(\mathbf{x}, t)$ is also affected by the density, HHD should be applied to $\mathbf{u}'(\mathbf{x}, t)$, followed by computation of the velocities $\mathbf{u}_s''$ and $\mathbf{u}_p''$ using Eq. (11), i.e.,

$$u_{s,i}'' \equiv u_{s,i}' - \widetilde{u_{s,i}'}, \qquad u_{p,i}'' \equiv u_{p,i}' - \widetilde{u_{p,i}'}. \tag{12}$$

Subsequently, contributions of the solenoidal and potential velocity fields to the Favre-averaged Reynolds stress term can be evaluated as follows

$$\frac{\partial}{\partial x_k}\overline{\rho u_i'' u_k''} = \underbrace{\frac{\partial}{\partial x_k}\overline{\rho u_{s,i}'' u_{s,k}''}}_{T_1} + \underbrace{\frac{\partial}{\partial x_k}\overline{\rho u_{p,i}'' u_{p,k}''}}_{T_2} + \underbrace{\frac{\partial}{\partial x_k}\overline{\rho u_{p,i}'' u_{s,k}''} + \frac{\partial}{\partial x_k}\overline{\rho u_{s,i}'' u_{p,k}''}}_{T_3}, \tag{13}$$

where $u_{s,i}''$ and $u_{p,i}''$ are defined by Eq. (12). Various terms in Eqs. (6) and (13) will be compared in Sect. IV by analyzing DNS data obtained from two flames characterized by different Ka.

Note that the Favre-averaged convection term is also affected by fluctuating solenoidal and potential velocities. Indeed, substitution of $\tilde{u}_i = \overline{\bar{u}_i + u_i'} = \bar{u}_i + \widetilde{u_i'}$ into a product of $\tilde{u}_i\tilde{u}_k$, followed by application of HHD to the fields $\bar{\mathbf{u}}(\mathbf{x}, t)$ and $\mathbf{u}'(\mathbf{x}, t)$ results in a sum of 16 terms. In the statistically 1D and planar case, $\bar{u}_{p,1} = \bar{u}_1$, $\bar{u}_{s,1} = 0$, and

$$\frac{\partial}{\partial x_1}(\bar{\rho}\tilde{u}_1^2) = \underbrace{\frac{\partial}{\partial x_1}\left(\bar{\rho}\widetilde{u_{s,1}'u_{s,1}'}\right)}_{T_1} + \underbrace{2\frac{\partial}{\partial x_1}\left(\bar{\rho}\widetilde{u_{s,1}'}\bar{u}_1\right)}_{T_2} + \underbrace{2\frac{\partial}{\partial x_1}\left(\bar{\rho}\widetilde{u_{s,1}'u_{p,1}'}\right)}_{T_3}$$
$$+ \underbrace{\frac{\partial}{\partial x_1}(\bar{\rho}\bar{u}_1^2)}_{T_4} + \underbrace{2\frac{\partial}{\partial x_1}\left(\bar{\rho}\widetilde{u_{p,1}'}\bar{u}_1\right)}_{T_5} + \underbrace{\frac{\partial}{\partial x_1}\left(\bar{\rho}\widetilde{u_{p,1}'u_{p,1}'}\right)}_{T_6}. \quad (14)$$

III. NUMERICAL SIMULATIONS

A. DNS conditions

As the DNS attributes and data were reported earlier,[11,15,46-48] only a brief description is given below, with more details being reported in Appendix A. Unconfined statistically 1D and planar, lean (the equivalence ratio Φ=0.7) H_2-air turbulent flames were investigated by (i) adopting a detailed (9 species, 23 reversible reactions) chemical mechanism[49] with the mixture-averaged transport model and (ii) numerically solving unsteady three-dimensional governing equations, written in compressible form. Note that while differential diffusion effects are well known to be highly pronounced in very lean H_2-air flames and to significantly increase turbulent burning velocity, as reviewed elsewhere,[38] differential diffusion was shown[50,51] to weakly affect a mean bulk burning rate at Φ=0.7. For this reason, the equivalence ratio was set equal to 0.7 in the present study.

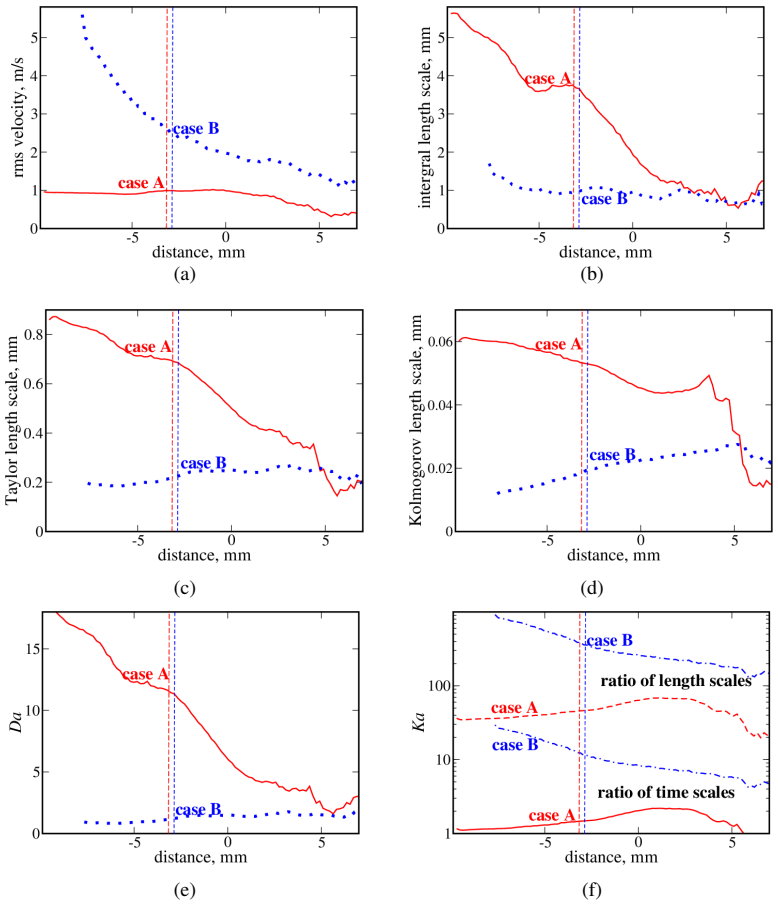

FIG. 1. Axial variations of turbulent flame characteristics conditioned to unburned mixture in flames A (red lines) and B (blue lines). Vertical dotted-dashed lines show the flame-brush leading edge, i.e., planes characterized by $\widetilde{c(\xi)} = 0.05$. (a) rms turbulent velocity u', (b) integral length scale $L_{k\varepsilon}$, (c) Taylor microscale λ, (d) Kolmogorov length scale η_K, (e) Damköhler number, (f) Karlovitz number $Ka = \tau_f/\tau_K$ and $(\delta_L/\eta_K)^2$.

Two cases A and B, characterized by two different values of the inlet rms velocity, with all other things being equal, were studied. Variations of the major turbulence characteristics along the x-axis in these two cases are shown in Fig. 1. Here, the distance ξ is counted from a transverse plane characterized by $\langle c \rangle(x,t) = 0.5$ at each instant, i.e., $\langle c \rangle(\xi,t) = 0.5$; the

combustion progress variable c is defined using fuel mass fraction; all reported quantities $\langle \cdot | c < 0.02 \rangle$ are conditioned to unburned mixture, i.e., to $c(\mathbf{x}, t) < 0.02$, and, subsequently, are transverse and time-averaged; $u' = \sqrt{2\langle u_k' u_k' | c < 0.02 \rangle / 3}$; $L_{k\varepsilon} = \langle 0.5 u_k' u_k' | c < 0.02 \rangle^{3/2} / \langle \varepsilon | c < 0.02 \rangle$; $Da = L_{k\varepsilon} S_L / (u' \delta_L)$; $Ka = \tau_f / \tau_K$, with a ratio of $(\delta_L / \eta_K)^2$ being also plotted in Fig. 1f; $\tau_K = (\nu_u / \langle \varepsilon | c < 0.02 \rangle)^{1/2}$ and $\eta_K = (\nu_u^3 / \langle \varepsilon | c < 0.02 \rangle)^{1/4}$; $\lambda = 15 \nu_u u'^2 / \langle \varepsilon | c < 0.02 \rangle$ is Taylor microscale; and the local dissipation rate $\varepsilon = 2\nu_u S_{jk} S_{jk}$. A slow decrease in η_K with the streamwise distance near the leading edge of flame A (see red solid line in Fig. 1d) is attributed to the influence of combustion-induced thermal expansion on turbulence upstream of the flame, as will be discussed later (see Fig. 7a in Sect. IV).

Table I. Relevant parameters characterizing the DNS cases.

	u_0'/S_L	L_T/δ_L	Re_T	u'/S_L	$L_{k\varepsilon}/\delta_L$	Da	Ka	$(\delta_L/\eta_K)^2$	Da_{cr}
A	0.7	14	227	0.7	10.3	11	1.5	46	0.11
B	5.0	14	1623	1.9	2.7	1.2	12	385	0.03

Major characteristics of the injected turbulence and major turbulent flame characteristics evaluated at the leading edges of the two flame brushes are reported in Table I. Here, u_0' is the rms velocity in the injected flow; L_T is the most energetic length scale of the Passot-Pouquet spectrum;[52] $Re_T = u_0' L_T / \nu_u$; the quantities u', $L_{k\varepsilon}$, Da, and Ka have been sampled at $\overline{c(\xi)} = 0.05$; $S_L = 1.36$ m/s, $\delta_L = 0.36$ mm, $\sigma = 6.7$, and, hence, $Ka_{cr}^B = 5.7$ have been computed under the simulation conditions (atmospheric pressure and $T_u = 300$ K); Da_{cr} has been calculated using Eq. (7) and the DNS data on $\delta_t = (T_b - T_u)/\max|\nabla \bar{T}|$, whereas Eq. (10) yields $Da_{cr} = 0.03$ for both flames. In case B, Eqs. (7) and (10) yield close results. In case A, the Damköhler number is significantly higher; consequently, scaling of $\delta_t \propto \delta_L \sqrt{Re_T}$ does not hold and results yielded by Eqs. (7) and (10) are different. Note also that $(\delta_L/\eta_K)^2$ is

much larger than $Ka = \tau_f/\tau_K$, because $\delta_L = (T_b - T_u)/\max|\nabla T| \gg \nu_u/S_L$ in the studied complex-chemistry case.

The criteria introduced in Sect. II, both Eq. (7) and Eq. (10), imply that combustion-induced thermal expansion can substantially affect the large-scale turbulence characteristics in both flames A and B. On the contrary, Eq. (2) suggests that the influence of the thermal expansion on the small-scale turbulence characteristics can be of importance in flame A only, whereas $Ka > Ka_{cr}^B$ in case B.

When processing the DNS data, transverse-averaged quantities $\langle\cdot\rangle(\xi,t)$ were sampled first, followed by time-averaging of them. Time and transverse-averaged quantities are designated with overbar, e.g., $\bar{c}(\xi) \equiv \overline{\langle c\rangle(\xi,t)}$.

B. Helmholtz-Hodge decomposition

The fluctuating velocity $\mathbf{u}'(\mathbf{x},t)$ was decomposed into solenoidal and potential components $\mathbf{u}_s'(\mathbf{x},t)$ and $\mathbf{u}_p'(\mathbf{x},t)$ by using two methods: (i) conventional[33] HHD and (ii) natural[53,54] decompositions. To do so, algorithms that were applied earlier by the present authors to velocity fields obtained from weakly turbulent single-step chemistry flames[55,56] and from flames[15] A and B were adopted. The reader interested in a detailed discussion of these algorithms is referred to the latter paper.[15] Since the earlier results yielded by the two decompositions were hardly distinguishable within flame brushes,[55] we will report results obtained using the former method only.

The fields $\mathbf{u}_s''(\mathbf{x},t)$ and $\mathbf{u}_p''(\mathbf{x},t)$ were computed using Eq. (12). Note that $\nabla\cdot\mathbf{u}_s'' \neq 0$ and $\nabla\times\mathbf{u}_p'' \neq 0$.

IV. NUMERICAL RESULTS AND DISCUSSION

To obtain Eqs. (7) and (10) in Sect. II, two assumptions were invoked: (i) correlation between solenoidal velocity fluctuations and dilatation did not vanish and (ii) the order of magnitude of local dilatation in turbulent premixed flames could be estimated using the laminar-flame value Θ. These assumptions are validated in Figs. 2 and 3, respectively.

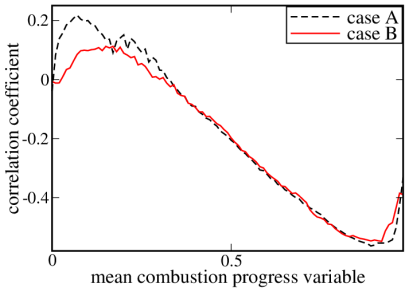

FIG. 2. Correlation coefficient $\overline{u'_{s,1}\nabla\cdot\mathbf{u}'_p}/\left[\overline{u'^2_{s,1}}\,\overline{(\nabla\cdot\mathbf{u}'_p)^2}\right]^{1/2}$ vs. mean combustion progress $\tilde{c}$.

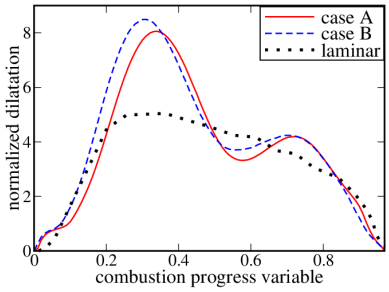

FIG. 3. Conditioned dilatation $\langle\nabla\cdot\mathbf{u}|c\rangle$ sampled from the entire computational domain in case A or B, as well as dependence of $\nabla\cdot\mathbf{u}$ on c in the counterpart laminar flame.

More specifically, Fig. 3 shows that the conditioned dilatation $\langle\nabla\cdot\mathbf{u}|c\rangle$ is indeed on the order of $\nabla\cdot\mathbf{u}(c)$ in the laminar flame, while the former can be larger than the latter. A similar quantitative difference was reported in earlier DNS studies.[36,37] Such a difference can be

controlled by three physical mechanisms: (i) local flame thinning due to turbulent stretch rates, (ii) local flame broadening due to small-scale turbulent mixing, and (iii) differential diffusion effects if molecular transport coefficients for fuel, oxidant, and heat are substantially different. Mechanisms (i) and (ii) always compete and can either decrease or increase the local flame thickness depending on conditions.[57] Accordingly, the local dilatation is either increased or decreased, respectively. Differential diffusion effects can change not only the local flame thickness but also the local normal velocity jump at the flame. While for the considered mixture, mean bulk burning rate was shown to be weakly affected by differential diffusion, variations in the local flame characteristics were also documented.[50,51] Further discussion of Fig. 3 is beyond the scope of the present work, and differences between the turbulent $\langle \nabla \cdot \mathbf{u} | c \rangle$, see solid and dashed lines, and the laminar $\nabla \cdot \mathbf{u}(c)$, see dotted line, could be addressed in a future study.

Figure 4 shows variations of all terms in Eq. (6) within mean flame brushes. Note that the almost perfect agreement between the LHS and RHS of this equation in both cases, cf. black solid and brown dotted lines, verifies conservation in the simulations. Contrary to the criterion given by Eq. (2), but in line with the newly introduced criterion given by Eq. (7), thermal expansion effects are well pronounced not only in flame A, but also in flame B. More specifically, the magnitude of the last term (T_4), which contains dilatation and, hence, arises due to thermal expansion, is comparable with or larger than the magnitude of the purely solenoidal term T_1. Furthermore, at $\bar{c} > 0.5$, the former term dominates within both flames, i.e., $|T_4|$ is much larger than $|T_1 + T_2 + T_3|$. These DNS data clearly show importance of thermal expansion effects under conditions of the present study, thus, supporting the analysis in Sect. II. Note that (i) $T_4 < 0$ at $\bar{c} > 0.5$ because dilatation reduces vorticity in flames,[16-19] i.e., correlation between solenoidal velocity fluctuations and dilatation is predominantly

304 negative (see Fig. 2); but (ii) the RHS of Eq. (6) is positive because it includes T_4 with a minus
305 sign.

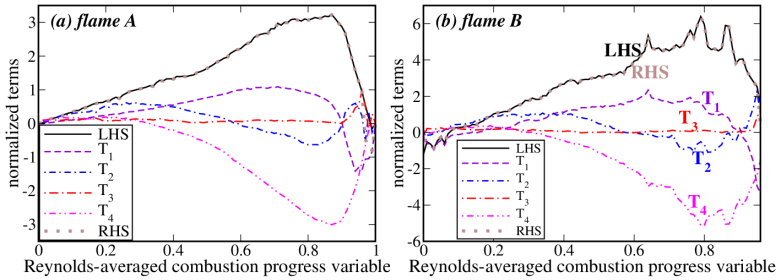

306
307 **FIG. 4.** Various terms in Eq. (6), normalized using S_L and δ_L, in flames (a) A and (b) B.

308 Importance of thermal expansion effects is also shown in Fig. 5, which reports various terms
309 in Eq. (13) for the two statistically one-dimensional planar flames (note almost perfect
310 matching between the LHS and RHS again). Although the magnitude of the solenoidal term
311 T_1 is larger than the magnitudes of other terms at $\bar{c} > 0.5$ in both flames and at $\bar{c} < 0.2$ in
312 flame B, term T_3, which involves both solenoidal and potential velocities, also plays an
313 important role. Even the potential term T_2 is not negligible.

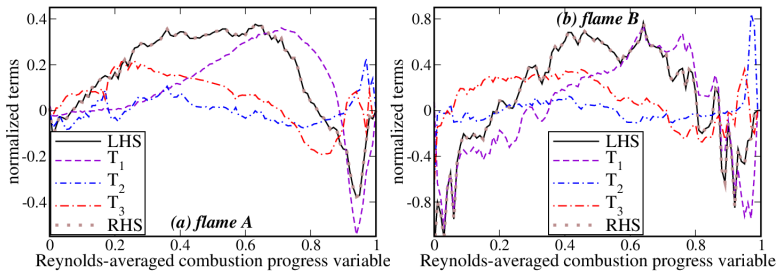

314
315 **FIG. 5.** Various terms in Eq. (13), normalized using ρ_u, S_L, and δ_L, in flames (a) A and (b) B.

316 At the same time, comparison of Figs. 4 and 5 indicates that thermal expansion effects are
317 less pronounced within the Favre-averaging framework, i.e., the dilatation term (T_4)

dominates at $\bar{c} > 0.5$ on the RHS of Eq. (6), whereas the solenoidal term (T_1) is the most important term on the RHS of Eq. (13) in the largest parts of the two flame brushes. However, this result does not mean that the use of Favre-averaged velocities is favorable in solving the problem of modeling turbulence in flames. The fact that the solenoidal term is the largest term on the RHS of Eq. (13) at $\bar{c} > 0.5$ does not prove that models developed for solenoidal incompressible turbulent flows hold for the solenoidal term on the RHS of Eq. (13) in flames. Rather, combustion-induced thermal expansion can substantially affect not only potential velocity fluctuations, but also solenoidal turbulence even at high Ka. Two examples follow.

First, Fig. 3 and a large magnitude of term T_4 on the RHS of Eq. (6) (see Fig. 4) show a well-pronounced negative (at $\bar{c} > 0.4$) correlation between dilatation and solenoidal velocity fluctuations, thus implying a substantial influence of thermal expansion on the solenoidal velocity field in the studied flames.

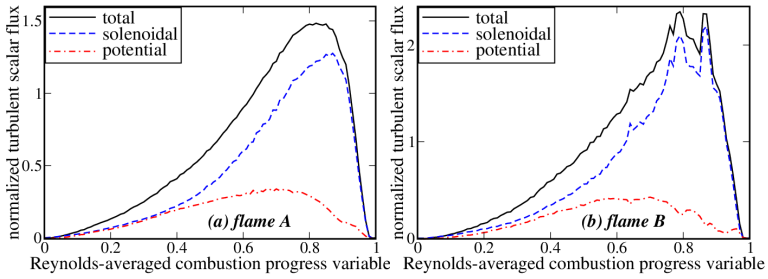

FIG. 6. Axial turbulent scalar flux normalized using ρ_u and S_L in flames (a) A and (b) B.

Second, Fig. 6 shows that not only the total turbulent scalar flux $\overline{\rho u'' c''}$, but also its solenoidal and potential components are counter-gradient ($d\bar{c}/dx > 0$ in the studied flames). The counter-gradient behavior of $\overline{\rho u_s'' c''}$ indicates a substantial influence of thermal expansion on the solenoidal velocity in the considered flames. This influence is attributed to vorticity that is generated by baroclinic torque. As discussed in detail elsewhere,[6,8] such a

337 vorticity acts to push the leading and trailing segments of the instantaneous flame inside the
338 mean flame brush. Thus, for a flame propagating from right to left, fluctuations in the local
339 u_s, caused by baroclinic torque, are positive and negative at $\bar{c} \ll 1$ and $1-\bar{c} \ll 1$,
340 respectively. Fluctuations in the local c, caused by appearance of the instantaneous flame, are
341 also positive and negative in these zones, respectively. Therefore, u_s' correlates positively with
342 c'. It is worth noting that the obtained counter-gradient behavior of the flux $\overline{\rho u'' c''}$ does not
343 contradict the well-known Bray number criterion,[26,27] because $u'/S_L < \sigma - 1$ even in case B.
344 As evidenced by the above analysis, there is substantial influence of combustion-induced
345 thermal expansion not only on the total and potential velocity fluctuations, but also on the
346 solenoidal velocity fluctuations at $Ka = \tau_f/\tau_K$ as large as 12 and $(\delta_L/\eta_K)^2$ about 400.

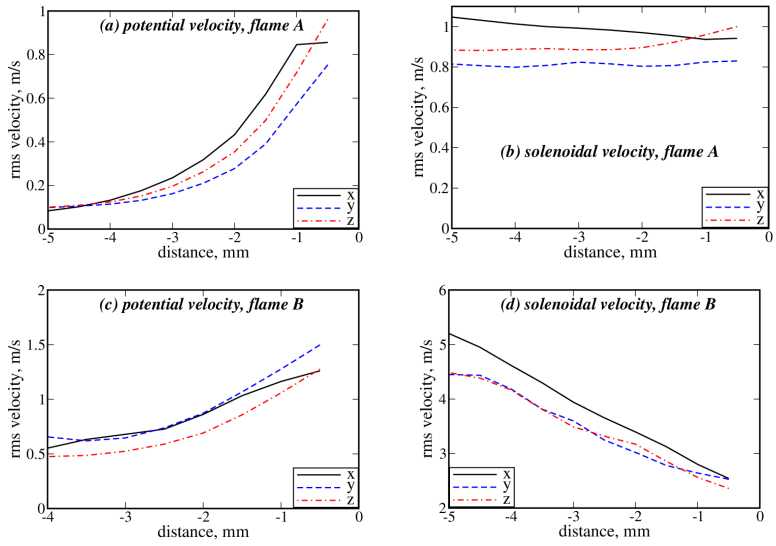

FIG. 7. Variations of (a), (c) potential and (b), (d) solenoidal rms velocities $\left(\overline{u_{i,p}'^2}\right)^{1/2}$ and $\left(\overline{u_{i,s}'^2}\right)^{1/2}$, respectively, upstream of flames (a)-(b) A and (c)-(d) B. Zero distance corresponds to $\langle c \rangle(x,t) = 0.01$.

347

348

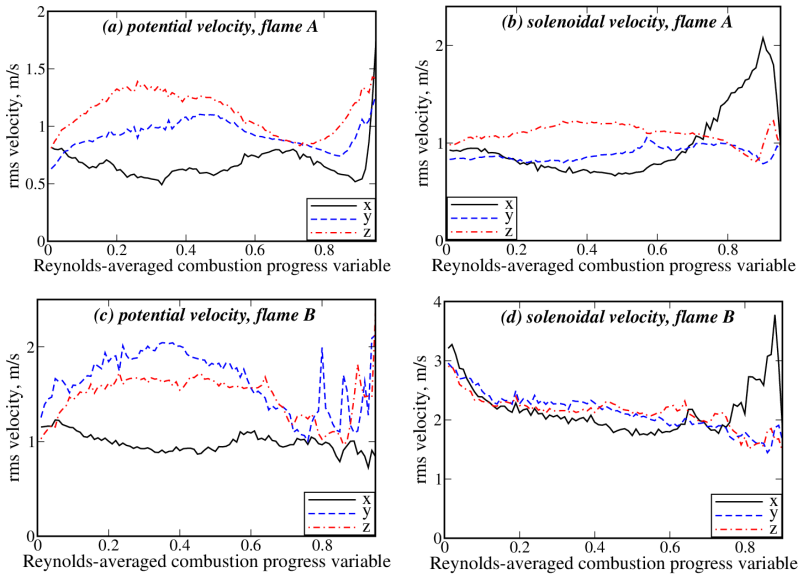

FIG. 8. Variations of (a), (c) potential and (b), (d) solenoidal rms velocities conditioned to unburned mixture, i.e., $\overline{\langle u_{i,p}'^2 | c(\mathbf{x},t) < 0.01 \rangle}^{1/2}$ and $\overline{\langle u_{i,s}'^2 | c(\mathbf{x},t) < 0.01 \rangle}^{1/2}$, respectively, within flames (a)-(b) A and (c)-(d) B.

349 Further insights into the influence of combustion-induced thermal expansion on turbulence
350 in flames can be obtained from Figs. 7 and 8. In particular, Figs. 7a and 7c show that the rms
351 magnitude $\left(\overline{u_{i,p}'^2}\right)^{1/2}$ of the potential velocity fluctuations increases upstream of the flame
352 brush as the flow approaches the flame leading edge $\langle c \rangle(x,t) = 0.01$. This effect is attributed
353 to generation of potential velocity fluctuations by combustion-induced pressure perturbations
354 that propagate upstream of the flame. A similar physical mechanism is well known to cause
355 the hydrodynamic instability of laminar premixed flames.[58,59] On the contrary, the solenoidal
356 $\left(\overline{u_{i,s}'^2}\right)^{1/2}$ decreases with distance from the inlet due to turbulence decay, which is much more
357 pronounced in the highly turbulent case B. As a result, the potential and solenoidal rms

velocities are comparable in the region close to the flame leading edge, cf. rightmost points on curves in Figs. 7a and 7b for case A, and Figs. 7c and 7d for case B.

Last, Fig. 8 shows that rms values of potential and solenoidal velocity fluctuations, conditioned to unburned gas are comparable with one another within A or B-flame brush.

V. TURBULENCE-IN-PREMIXED-FLAME DIAGRAM

The goal of this section is to discuss different criteria of importance of thermal expansion effects in premixed flames and to present such criteria in a regime diagram. While this diagram seems similar to the classical premixed-turbulent-combustion regime-diagrams,[60-62] there is an important difference: the classical diagrams address the influence of turbulence on a premixed flame, whereas the present diagram considers the influence of a premixed flame on turbulence.

First, let us compare the two criteria given by Eqs. (2) and (10). Using the well-known scaling of $Da^2Ka^2 \propto Re_t = u'L/\nu$, where constants of unity order are omitted for brevity, the critical number Da_{cr} could be substituted with $\sqrt{Re_t}/Ka_{cr}$. Accordingly, Eq. (10) reads

$$Ka_{cr} = (\sigma-1)^2\sqrt{Re_t} = Ka_{cr}^B(\sigma-1)\sqrt{Re_t} \gg Ka_{cr}^B. \quad (15)$$

Alternatively, Eq. (2) can be rewritten as follows

$$Da_{cr}^B = \sqrt{Re_t}(\sigma-1)^{-1} = (\sigma-1)\sqrt{Re_t}Da_{cr} \gg Da_{cr}. \quad (16)$$

Thus, the newly introduced criterion substantially extends the domain of the influence of combustion-induced thermal expansion on turbulence in premixed flames to a higher Karlovitz number and a lower Damköhler number. The DNS data analyzed in Sect. IV and, in particular, Figs. 4, 5, 7, and 8 are consistent with this extension.

Second, as noted in Sect. I, O'Brien et al.[28] have theorized that backscatter can arise from smaller scales, associated with injection of kinetic energy due to combustion, to larger scales whose lifetime τ_m is shorter than or equal to the laminar flame time scale τ_f. In the inertial range[29] of Kolmogorov turbulence, a constraint of $\tau_m \leq \tau_f$ reads $(l_m^2/\bar{\varepsilon})^{1/3} \leq \tau_f$ or

$$l_m \leq \left(\bar{\varepsilon}\tau_f^3\right)^{1/2} = S_L^{-3/2}\delta_L^{3/2}(\nu_u/\tau_K^2)^{1/2} = \delta_L Ka\Gamma^{-1/2}, \qquad (17)$$

with the length scale $\left(\bar{\varepsilon}\tau_f^3\right)^{1/2}$ being earlier introduced by Corrsin.[63] Here, the number $\Gamma \equiv S_L\delta_L/\nu_u$, known as "flame Reynolds number", is larger than unity and can be as large as 50 in lean hydrogen-air mixtures under room conditions.[64] If the energy flux due to combustion is localized to scales on the order of δ_L,[65-67] the scale l_m should be larger than δ_L. Therefore, Eq. (17) implies that backscatter could arise if $Ka\Gamma^{-1/2} > 1$ or

$$Ka > \Gamma^{1/2}. \qquad (18)$$

If $Ka < \Gamma^{1/2}$, even the smallest turbulent eddies evolve slowly, such that combustion-induced local velocity perturbations are associated with rapid distortion within the flame, and "any cascade interaction through convective transport between small and large scales is relegated to the far wake of the burnt gases."[32]

Equation (17) is a necessary condition for existence of a spectral interval where backscatter can be induced by combustion. However, to cause backscatter, combustion should be sufficiently strong. By extending Bilgers' arguments,[28] let us hypothesize that backscatter may arise if the dilatation Θ is larger than the magnitude of turbulence-induced velocity gradient $(\delta_L^2/\bar{\varepsilon})^{-1/3}$ at the scale $l = \delta_L$, associated with the energy injection due to combustion. Here, this length scale is assumed to belong to the inertial range of turbulence spectrum, which seems to be plausible if $Ka > Ka_{cr}^B > 1$ (especially for lean hydrogen-air mixtures, where

$\delta_L/\eta_K \gg Ka^{1/2}$ under room conditions). Therefore, backscatter may arise in the inertial range if

$$\Theta(\delta_L^2/\bar{\varepsilon})^{1/3} = (\sigma-1)S_L\delta_L^{-1/3}(\tau_K^2/\nu_u)^{1/3} = (\sigma-1)Ka^{-2/3}(S_L\delta_L/\nu_u)^{1/3} > 1 \quad (19)$$

or

$$Ka < Ka_{cr}^* = (\sigma-1)^{3/2}\Gamma^{1/2} = (\sigma-1)^{1/2}\Gamma^{1/2}Ka_{cr}^B. \quad (20)$$

Since $Ka_{cr}^* > Ka_{cr}^B$ and $\Gamma^{1/2} < Ka_{cr}^B$ for most fuels (or $\Gamma^{1/2} \cong Ka_{cr}^B$ in lean hydrogen-air mixtures), Eqs. (18) and (20) are consistent with one another. Under conditions of $\Gamma^{1/2} < Ka < Ka_{cr}^*$, both $\Gamma^{1/2} < Ka < Ka_{cr}^B$ and $\Gamma^{1/2} < Ka_{cr}^B < Ka$ are possible, i.e., Eq. (2) may or may not hold. Thus, backscatter may arise even if the smallest-scale turbulent eddies are weakly affected by combustion-induced thermal expansion.

For the present flame B, $Ka = 12$ (see Table I) is larger than $Ka_{cr}^B = 5.7$, but is smaller than $Ka_{cr}^* = 75$. Accordingly, substantial influence of combustion-induced thermal expansion on turbulent eddies from the inertial range is expected. Indeed, two-point second-order structure functions for the potential velocity field, which (i) were sampled from flame B, (ii) were conditioned to unburnt mixture, and (iii) were reported in a recent paper,[15] do show such an influence even at small distances r between two points where velocity is picked. In flame A characterized by $Ka < Ka_{cr}^B$, the effect is observed even at very small r, cf. Figs. 4b and 4e or 4c and 4f in the cited paper, where flames A and B are labeled with letters W and H, respectively.

Using a scaling of $Da^2Ka^2 \propto Re_t$, Eq. (20) reads

$$Da > Da_{cr}^* = \sqrt{Re_t}(\sigma-1)^{-3/4}\Gamma^{-1/4} = \sqrt{Re_t}(\sigma-1)^{5/4}\Gamma^{-1/4}Da_{cr}. \quad (21)$$

Therefore, $Da_{cr}^{*} > Da_{cr}$ if $Re_t > (\sigma-1)^{-5/2}\Gamma^{1/2}$, which holds in a turbulent flow, where $Re_t \gg 1$. Thus, when compared to Eq. (20), which allows for backscatter in the inertial range, the newly introduced criterion given by Eq. (10) substantially extends the domain of the influence of combustion-induced thermal expansion on turbulence in premixed flames to a lower Damköhler number.

In addition to the three criteria given by Eqs. (2), (10), and (20), one more criterion is worth mentioning. Hydrodynamic instability of laminar premixed flames[58,59] stems from velocity perturbations upstream of the flame, caused by combustion-induced pressure waves. Thus, the instability is an example of the discussed thermal expansion effects. However, as shown elsewhere,[38,68-70] the instability plays a minor role in premixed turbulent combustion if Ka is of unity order or larger. Therefore, the instability cannot change the three criteria given by Eqs. (2), (10), and (20).

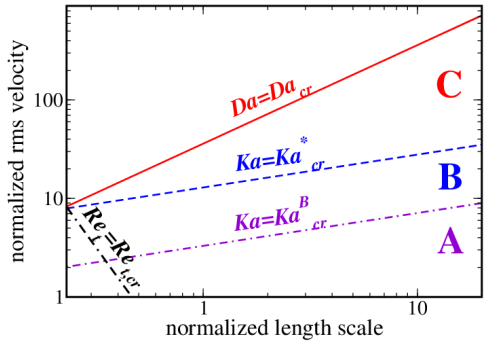

FIG. 9. Turbulence-in-premixed-flame diagram $\{L/\delta_L, u'/S_L\}$ sketched using Eq. (2) (violet dotted-dashed line), Eq. (10) (red solid line), Eq. (20) (blued dashed line), and Eq. (22) (black double-dashed-dotted line). $\sigma = 7$, $\Gamma = 10$, and $u'/S_L = Ka^{2/3}(L/\delta_L)^{1/3}$. A: region of the influence of thermal expansion on small-scale turbulence. B: active cascade region. C: region of the influence of thermal expansion on large-scale turbulence.

The three criteria given by Eqs. (2), (10), and (20) are plotted in violet dotted-dashed, red solid, and blue dashed lines, respectively, in Fig. 9. To do so, values of $\sigma = 7$ and $\Gamma = 10$,

associated with near-stoichiometric methane-air mixtures under room conditions, were set and the following simplified relation $u'/S_L = Ka^{2/3}(L/\delta_L)^{1/3}$ was invoked. Since Eq. (10) was obtained using Eq. (7) and the following scaling $\delta_{t,\infty}/L \propto Re_t^{1/2}$, extrapolation of Eq. (10) to low length scale ratios L/δ_L is limited by a constraint of $\delta_{t,\infty} > \delta_L$ or

$$Re_t > Re_{t,cr} = \left(\frac{\delta_L}{L}\right)^2. \quad (22)$$

In Fig. 9, this constraint is plotted in black double-dashed-dotted line.

In the domain bounded by Eqs. (10) and (20), combustion-induced thermal expansion can affect large-scale turbulence characteristics, as discussed in Sects. III and V. In a band bounded by Eqs. (2) and (20), the combustion-induced thermal expansion can also cause backscatter in the inertial range of turbulence spectrum. Following O'Brien et al.,[32] this layer is labeled "active cascade". Note that Eq. (18) holds for the selected values of $\sigma = 7$ and $\Gamma = 10$. Finally, below the violet dotted-dashed line yielded by Eq. (2), the combustion-induced thermal expansion can also affect the smallest turbulent eddies.

VI. CONCLUSIONS

A new criterion was introduced for assessing importance of turbulence modulations due to combustion-induced thermal expansion in premixed flames. The criterion highlights a ratio of dilatation in the laminar flame to the large-scale gradient of rms turbulent velocity across the turbulent flame brush. When compared to the well-known Bilger's criterion,[28] the developed criterion substantially expands domain of conditions associated with importance of thermal expansion. It is worth stressing, however, that the present study extends Bilger's analysis,[28] rather than contradicting it. The point is that Bilger[28] addressed the influence of combustion-

induced thermal expansion on small-scale turbulence characteristics, whereas the present work allows for large-scale effects.

Assumptions invoked to arrive to the newly introduced criterion were validated by analyzing DNS data obtained earlier from two complex-chemistry, lean H_2-air flames propagating in a box. In line with the new criterion, results show significant influence of combustion-induced potential velocity fluctuations on evolution of the second moments of the turbulent velocity field upstream of and within both flame brushes. In particular, the DNS data show that (i) potential and solenoidal rms velocities are comparable in unburnt gas close to the leading edge of flame brush in each case and (ii) potential and solenoidal rms velocities conditioned to unburnt gas are comparable within entire flame brush in each case.

Moreover, the DNS data indicate that combustion-induced thermal expansion affects not only total and potential velocities, but also solenoidal velocity. Such effects manifest themselves in a negative correlation between the solenoidal velocity fluctuations and dilatation or in the counter-gradient behavior of the solenoidal scalar flux $\overline{\rho u_s'' c''}$. Therefore, the applicability of constant-density turbulence models to the solenoidal velocity fluctuations in flames may be subjected to scrutiny even at $(\delta_L/\eta_K)^2$ about 400.

To summarize results of earlier relevant studies[10,28,32] and the present one, various regimes of the influence of combustion-induced thermal expansion on turbulence spectrum in premixed flames are outlined in a newly introduced turbulence-in-premixed-flame (TiPF) diagram.

Declaration of Competing Interest

The authors declare that they have no known competing financial interests or personal relationships that could have appeared to influence the work reported in this paper.

Acknowledgements

V.A.S. gratefully acknowledges support provided by ONERA and by the Ministry of Science and Higher Education of the Russian Federation (Grant agreement of December 8, 2020 No. 075-11-2020-023) within the program for the creation and development of the World-Class Research Center "Supersonic" for 2020-2025. A.N.L. gratefully acknowledges the financial support provided by CERC and Chalmers Area of Advance "Transport". F.E.H.P. and H.G.I. were sponsored by King Abdullah University of Science and Technology (KAUST). Computational resources for the DNS calculations were provided by the KAUST Supercomputing Laboratory.

DATA AVAILABILITY

The data that support the findings of this study are available from the corresponding author upon reasonable request.

APPENDIX A: DNS ATTRIBUTES

Simulations were performed in a rectangular domain of size of 20×10×10 mm^3 using a uniform Cartesian mesh of 512×256×256 cells. The mesh ensured about ten grid points per δ_L, with Kolmogorov length scale being larger than cell size Δx. Unsteady three-dimensional partially differential transport equations were discretized using an eighth-order central difference scheme for internal mesh points, with the order of differentiation being gradually decreased to a one-sided fourth-order scheme near the inlet and outlet boundaries.[71] Time integration was performed adopting an explicit fourth-order Runge-Kutta scheme.[71]

Along the flame propagation direction, inflow and outflow characteristic boundary conditions were set using an improved Navier-Stokes characteristic boundary condition technique.[72] Other boundary conditions were periodic.

A divergence-free, isotropic, homogeneous turbulent velocity field was generated using a pseudo spectral method[73] and adopting the Passot-Pouquet spectrum.[52] The field was injected through the inlet (left) boundary and decayed along the mean flow direction (x-axis). At $t = 0$, a pre-computed planar laminar flame structure was embedded into the computational domain to initialize turbulent flame propagation from right to left along x-axis. Subsequently, the mean inlet flow velocity was gradually changed to match turbulent flame speed. Results reported in the present paper were sampled at six different instants in each case, i.e., at $t/t_e =$ 0.57, 0.67, 0.77, 0.86, 0.96, and 1.05 in case A and at $t/t_e = 4.1$, 4.8, 5.5, 6.2, 6.8, and 7.5 in case B, where, t_e is the eddy turnover time.

References

[1]B. Karlovitz, D. W. Denniston, and F. E. Wells, "Investigation of turbulent flames," J. Chem. Phys. **19**, 541-547 (1951).
[2]P. A. Libby and K. N. C. Bray, "Countergradient diffusion in premixed turbulent flames," AIAA J. **19**, 205-213 (1981).
[3]C. Dopazo, L. Cifuentes, and N. Chakraborty, "Vorticity budgets in premixed combusting turbulent flows at different Lewis numbers," Phys. Fluids **29**, 045106 (2017).
[4]Z. Wang and J. Abraham, "Effects of Karlovitz number on turbulent kinetic energy transport in turbulent lean premixed methane/air flames," Phys. Fluids **29**, 085102 (2017).
[5]A. N. Lipatnikov, V. A. Sabelnikov, S. Nishiki, and T. Hasegawa, "Combustion-induced local shear layers within premixed flamelets in weakly turbulent flows," Phys. Fluids **30**, 085101 (2018).
[6]A. N. Lipatnikov, V. A. Sabelnikov, S. Nishiki, and T. Hasegawa, "Does flame-generated vorticity increase turbulent burning velocity?" Phys. Fluids **30**, 081702 (2018).
[7]P. Brearley, U. Ahmed, N. Chakraborty, and A. N. Lipatnikov, "Statistical behaviours of conditioned two-point second-order structure functions in turbulent premixed flames in different combustion regimes," Phys. Fluids **31**, 115109 (2019).
[8]A. N. Lipatnikov, V. A. Sabelnikov, S. Nishiki, and T. Hasegawa, "A direct numerical simulation study of the influence of flame-generated vorticity on reaction-zone-surface area in weakly turbulent premixed combustion," Phys. Fluids **31**, 055101 (2019).
[9]A. R. Varma, U. Ahmed, and N. Chakraborty, "Effects of body forces on vorticity and enstrophy evolutions in turbulent premixed flames," Phys. Fluids **33**, 035102 (2021).
[10]J. F. MacArt and M. E. Mueller, "Damköhler number scaling of active cascade effects in turbulent premixed combustion," Phys. Fluids **33**, 035103 (2021).

[11]V. A. Sabelnikov, A. N. Lipatnikov, S. Nishiki, H. L. Dave, F. E. Hernández-Pérez, W. Song, and H. G. Im, "Dissipation and dilatation rates in premixed turbulent flames," Phys. Fluids **33**, 035112 (2021).
[12]N. Chakraborty, C. Kasten, U. Ahmed, and M. Klein, "Evolutions of strain rate and dissipation rate of kinetic energy in turbulent premixed flames," Phys. Fluids **33**, 125132 (2021).
[13]N. Chakraborty, U. Ahmed, M. Klein, and H. G. Im, "Alignment statistics of pressure Hessian with strain rate tensor and reactive scalar gradient in turbulent premixed flames," Phys. Fluids **34**, 065120 (2022).
[14]S. Kr. Ghai, N. Chakraborty, U. Ahmed and M. Klein, "Enstrophy evolution during head-on wall interaction of premixed flames within turbulent boundary layers," Phys. Fluids **34**, 075124 (2022).
[15]V. A. Sabelnikov, A. N. Lipatnikov, N. Nikitin, F. E. Hernández-Pérez, and H. G. Im, "Conditioned structure functions in turbulent hydrogen/air flames," Phys. Fluids **34**, 085103 (2022).
[16]A. N. Lipatnikov and J. Chomiak, "Effects of premixed flames on turbulence and turbulent scalar transport," Prog. Energy Combust. Sci. **36**, 1-102 (2010).
[17]V. A. Sabelnikov and A. N. Lipatnikov, "Recent advances in understanding of thermal expansion effects in premixed turbulent flames," Annu. Rev. Fluid Mech. **49**, 91-117 (2017).
[18]N. Chakraborty, "Influence of thermal expansion on fluid dynamics of turbulent premixed combustion and its modeling implications," Flow Turbul. Combust. **106**, 753-848 (2021).
[19]A.M. Steinberg, P. E. Hamlington, and X. Zhao, "Structure and dynamics of highly turbulent premixed combustion," Prog. Energy Combust. Sci. **85**, 100900 (2021).
[20]S. H. R. Whitman, C. A. Z. Towery, A. Y. Poludnenko, and P. E. Hamlington, "Scaling and collapse of conditional velocity structure functions in turbulent premixed flames," Proc. Combust. Inst. **37**, 2527-2535 (2019).
[21]J. Lee, J. F. MacArt, and M. E. Mueller, "Heat release effects on the Reynolds stress budgets in turbulent premixed jet flames at low and high Karlovitz numbers," Combust. Flame **216**, 1-8 (2020).
[22]R. Darragh, C. A. Z. Towery, A. Y. Poludnenko, and P. E. Hamlington, "Particle pair dispersion and eddy diffusivity in a high-speed premixed flame," Proc. Combust. Inst. **38**, 2845-2852 (2021).
[23]J. Lee and M. E. Mueller, "Closure modeling for the conditional Reynolds stresses in turbulent premixed combustion," Proc. Combust. Inst. **38**, 3031-3038 (2021).
[24]A. Kazbekov and A. M. Steinberg, "Flame- and flow-conditioned vorticity transport in premixed swirl combustion," Proc. Combust. Inst. **38**, 2949-2956 (2021).
[25]A. Kazbekov and A. M. Steinberg, "Physical space analysis of cross-scale turbulent kinetic energy transfer in premixed swirl flames," Combust. Flame **229**, 111403 (2021).
[26]K. N.C. Bray, "Turbulent transport in flames," *Proc. R. Soc. London* A **451**, 231-256 (1995).
[27]D. Veynante, A. Trouvé, K. N. C. Bray, and T. Mantel, "Gradient and counter-gradient scalar transport in turbulent premixed flames," J. Fluid Mech. **332**, 263-293.
[28]R. W. Bilger, "Some aspects of scalar dissipation," Flow, Turbul. Combust. **72**, 93-114 (2004).
[29]A. S. Monin and A. M. Yaglom, *Statistical Fluid Mechanics: Mechanics of Turbulence* (The MIT Press, Cambridge, Massachusetts, 1975), Vol. 2.
[30]J. F. MacArt, T. Grenga, and M. E. Mueller, "Effects of combustion heat release on velocity and scalar statistics in turbulent premixed jet flames at low and high Karlovitz numbers," Combust. Flame **191**, 468-485 (2018).
[31]J. F. MacArt, T. Grenga, and M. E. Mueller, "Evolution of flame-conditioned velocity statistics in turbulent premixed jet flames at varying Karlovitz number," Proc. Combust. Inst. **37**, 2503-2510 (2019).
[32]J. O'Brien, C. A. Z. Towery, P. E. Hamlington, M. Ihme, A. Y. Poludnenko, and J. Urzay, "The cross-scale physical-space transfer of kinetic energy in turbulent premixed flames," Proc. Combust. Inst. **36**, 1967-1975 (2017).
[33]A. J. Chorin and J. E. Marsden, *A Mathematical Introduction to Fluid Mechanics* (Springer, Berlin, Germany, 1993).
[34]V. A. Sabelnikov, R., Yu, and A. N. Lipatnikov, "Thin reaction zones in constant-density turbulent flows at low Damköhler numbers: Theory and simulations," Phys. Fluids **31**, 055104 (2019).

[35]J. F. Driscoll, J. H. Chen, A. W. Skiba, C. D. Carter, E. R. Hawkes, and H. Wang, "Premixed flames subjected to extreme turbulence: Some questions and recent answers," Prog. Energy Combust. Sci. **76**, 100802, (2020).
[36]N. Swaminathan, R. W. Bilger, and B. Cuenot, "Relationship between turbulent scalar flux and conditional dilatation in premixed flames with complex chemistry," Combust. Flame **126**, 1764-1779 (2001).
[37]N. Chakraborty and R. S. Cant, "Effects of Lewis number on scalar transport in turbulent premixed flames," Phys. Fluids **21**, 035110 (2009).
[38]A. N. Lipatnikov and J. Chomiak, "Molecular transport effects on turbulent flame propagation and structure," Prog. Energy Combust. Sci. **31**, 1-73 (2005).
[39]A. N. Lipatnikov and J. Chomiak, "Turbulent flame speed and thickness: Phenomenology, evaluation, and application in multi-dimensional simulations," Prog. Energy Combust. Sci. 28, 1-73 (2002).
[40]T. Sponfeldner, N. Soulopoulos, F. Beyrau, Y. Hardalupas, A. M. K. P. Taylor, and J. C. Vassilicos, "The structure of turbulent flames in fractal- and regular-grid-generated turbulence," Combust. Flame **162**, 3379-3393 (2015).
[41]J. Kim, A. Satja, R. P. Lucht, and J. P. Gore, "Effects of turbulent flow regime on perforated plate stabilized piloted lean premixed flames", Combust. Flame **211**, 158-172 (2020).
[42]S. Kheirkhah and Ö. L. Gülder, "A revisit to the validity of flamelet assumptions in turbulent premixed combustion and implications for future research," Combust. Flame **239**, 111635 (2022).
[43]R. Yu, X.-S. Bay, and A. N. Lipatnikov, "A direct numerical simulation study of interface propagation in homogeneous turbulence," J. Fluid Mech. **772**, 127-164 (2015).
[44]R. Yu and A.N. Lipatnikov, "Direct numerical simulation study of statistically stationary propagation of a reaction wave in homogeneous turbulence," Phys. Rev. E **95**, 063101 (2017).
[45]T. Kulkarni and F. Bisetti, "Analysis of the development of the flame brush in turbulent premixed spherical flames," Combust. Flame **234**, 111640 (2021).
[46]D. H. Wacks, N. Chakraborty, M. Klein, P. G. Arias, and H. G. Im, "Flow topologies in different regimes of premixed turbulent combustion: A direct numerical simulation analysis," Phys. Rev. Fluids **1**, 083401 (2016).
[47]A. N. Lipatnikov, V. A. Sabelnikov, F. E. Hernández-Pérez, W. Song, and H. G. Im, "A priori DNS study of applicability of flamelet concept to predicting mean concentrations of species in turbulent premixed flames at various Karlovitz numbers," Combust. Flame **222**, 370-382 (2020).
[48]A. N. Lipatnikov, V. A. Sabelnikov, F. E. Hernández-Pérez, W. Song, and H. G. Im, "Prediction of mean radical concentrations in lean hydrogen-air turbulent flames at different Karlovitz numbers adopting a newly extended flamelet-based presumed PDF," Combust. Flame **226**, 248-259 (2021).
[49]M. P. Burke, M. Chaos, Y. Ju, F. L. Dryer, and S. J. Klippenstein, "Comprehensive H_2/O_2 kinetic model for high-pressure combustion," Int. J. Chem. Kinet. **44**, 444-474 (2012).
[50]J. H. Chen and H. G. Im, "Stretch effects on the burning velocity of turbulent premixed hydrogen-air flames," Proc. Combust. Inst. **28**, 211-218 (2000).
[51]H. G. Im and J. H. Chen, "Preferential diffusion effects on the burning rate of interacting turbulent premixed hydrogen-air flames," Combust. Flame **131**, 246-258 (2002).
[52]T. Passot and A. Pouquet, "Numerical simulation of compressible homogeneous flows in the turbulent regime," J. Fluid Mech. **181**, 441-466 (1987).
[53]H. Bhatia, G. Norgard, V. Pascucci, and P.-T. Bremer, "The Helmholtz-Hodge decomposition – a survey," IEEE Trans. Vis. Comput. Graph. **19**, 1386-1404 (2013).
[54]H. Bhatia, V. Pascucci, and P.-T. Bremer, "The natural Helmholtz-Hodge decomposition for open-boundary flow analysis," IEEE Trans. Vis. Comput. Graph. **20**, 1566-1578 (2014).
[55]V. A. Sabelnikov, A. N. Lipatnikov, N. Nikitin, S. Nishiki, and T. Hasegawa, "Application of Helmholtz-Hodge decomposition and conditioned structure functions to exploring influence of premixed combustion on turbulence upstream of the flame," Proc. Combust. Inst. **38**, 3077-3085 (2021).
[56]V. A. Sabelnikov, A. N. Lipatnikov, N. Nikitin, S. Nishiki, and T. Hasegawa, "Solenoidal and potential velocity fields in weakly turbulent premixed flames," Proc. Combust. Inst. **38**, 3087-3095 (2021).

[57]R. Yu, T. Nillson, X.-S. Bai, and A. N. Lipatnikov, "Evolution of averaged local premixed flame thickness in a turbulent flow," Combust. Flame **207**, 232-249 (2019).
[58]L. D. Landau and E. M. Lifshitz, *Fluid Mechanics* (Pergamon Press, Oxford, 1987).
[59]Ya. B. Zel'dovich, G. I. Barenblatt, V. B. Librovich, and G. M. Makhviladze, *The Mathematical Theory of Combustion and Explosions* (Consultants Bureau, New York, 1985).
[60]R. Borghi, "On the structure and morphology of turbulent premixed flames," in *Recent Advances in Aerospace Science*, edited by S. Casci and C. Bruno (Plenum, New York, 1984), pp. 117-138.
[61]F. A. Williams, *Combustion Theory*, 2nd ed. (Benjamin/Cummings, Menlo Park, California, 1985).
[62]N. Peters, "Laminar flamelet concepts in turbulent combustion," Proc. Combust. Inst. **21**, 1231 (1986).
[63]S. Corrsin, "Reactant concentration spectrum in turbulent mixing with a first-order reaction," J. Fluid Mech. **11**, 407-416 (1961).
[64]A. N. Lipatnikov and V. A. Sabelnikov, "Karlovitz numbers and premixed turbulent combustion regimes for complex-chemistry flames," Energies **15**, 5840 (2022).
[65]H. Kolla, E. R. Hawkes, A. R. Kerstein, N. Swaminathan, and J. H. Chen, "On velocity and reactive scalar spectra in turbulent premixed flames," J. Fluid Mech. **754**, 456 (2014).
[66]A. N. Lipatnikov, J. Chomiak, V. A. Sabelnikov, S. Nishiki, and T. Hasegawa, "Influence of heat release in a premixed flame on weakly turbulent flow of unburned gas: a DNS Study," in *Proceedings of the 25th International Colloquium on the Dynamics of Explosions and Reactive Systems, 2-7 August 2015, Leeds, UK*, edited by M.I. Radulescu (University of Leeds, UK, 2015), paper 74.
[67]C. A. Z. Towery, A. Y. Poludnenko, J. Urzay, J. O'Brien, M. Ihme, and P. E. Hamlington, "Spectral kinetic energy transfer in turbulent premixed reacting flows," Phys. Rev. E **93**, 053115 (2016).
[68]H. Boughanem and A. Trouvé, "The domain of influence of flame instabilities in turbulent premixed combustion," Proc. Combust. Inst. **27**, 971-978 (1998).
[69]S. Chaudhuri, V. Akkerman, and C. K. Law, "Spectral formulation of turbulent flame speed with consideration of hydrodynamic instability," Phys. Rev. E **84**, 026322 (2011).
[70]N. Fogla, F. Creta, and M. Matalon, "The turbulent flame speed for low-to-moderate turbulence intensities: Hydrodynamic theory vs. experiments," Combust. Flame **175**, 155-169 (2017).
[71]H. G. Im, P. G. Arias, S. Chaudhuri, and H. A. Uranakara, "Direct numerical simulations of statistically stationary turbulent premixed flames," Combust. Sci. Technol. **188**, 1182 (2016).
[72]C. S. Yoo, Y. Wang, A. Trouve, and H. G. Im, "Characteristic boundary conditions for direct simulations of turbulent counterflow flames," Combust. Theor. Model. **9**, 617 (2005).
[73]R. S. Rogallo, Numerical Experiments in Homogeneous Turbulence, NASA Technical Memorandum 81315, NASA Ames Research Center, California, 1981.

PLEASE CITE THIS ARTICLE AS DOI: 10.1063/5.0123211

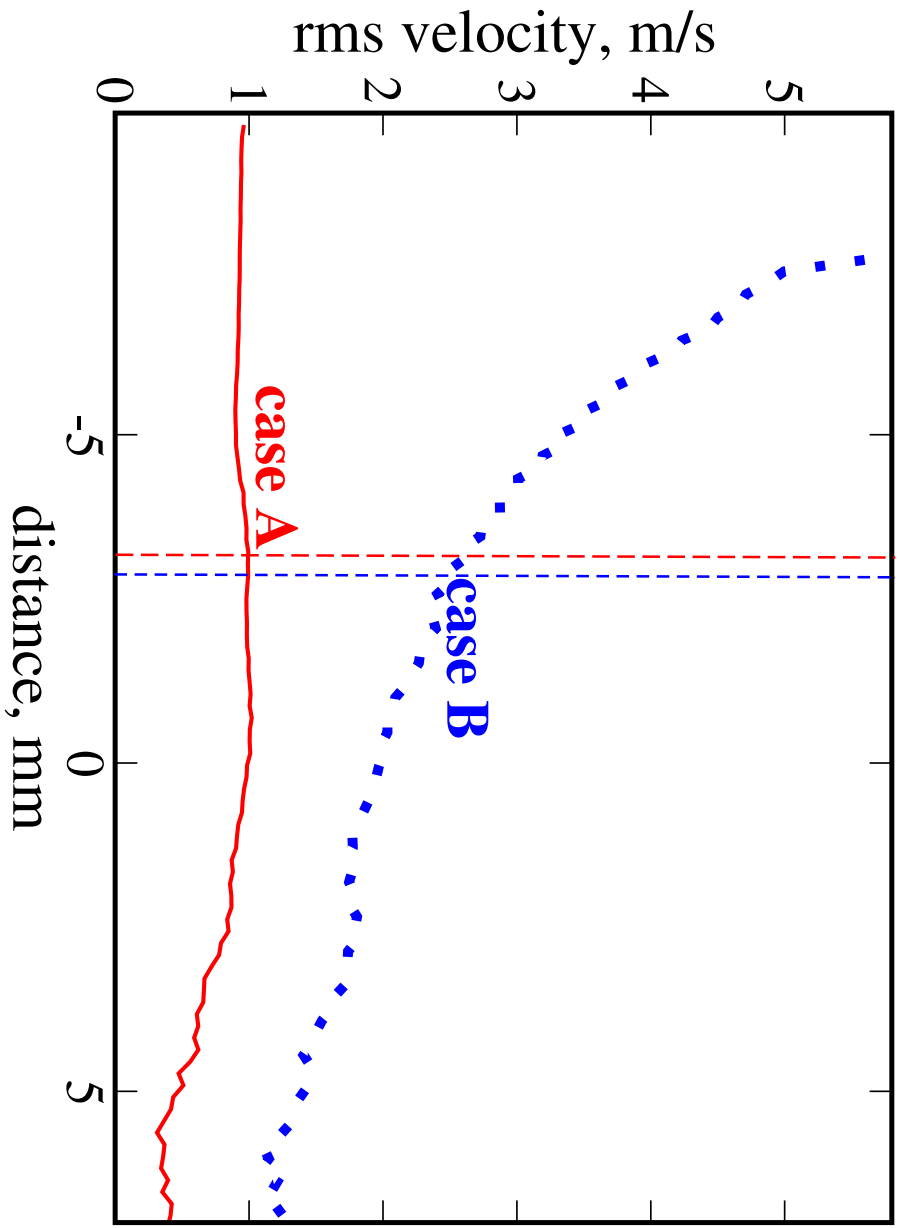

PLEASE CITE THIS ARTICLE AS DOI: 10.1063/5.0123211

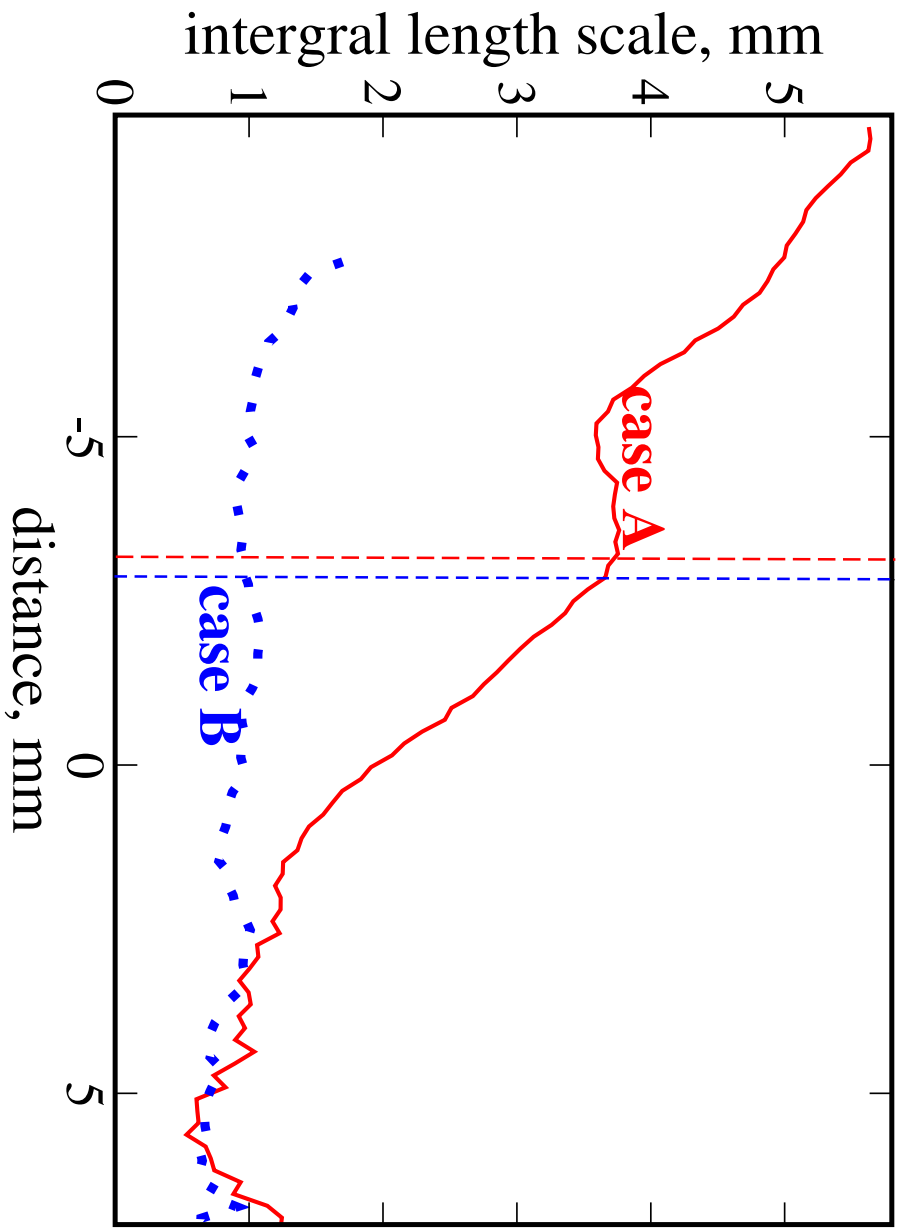

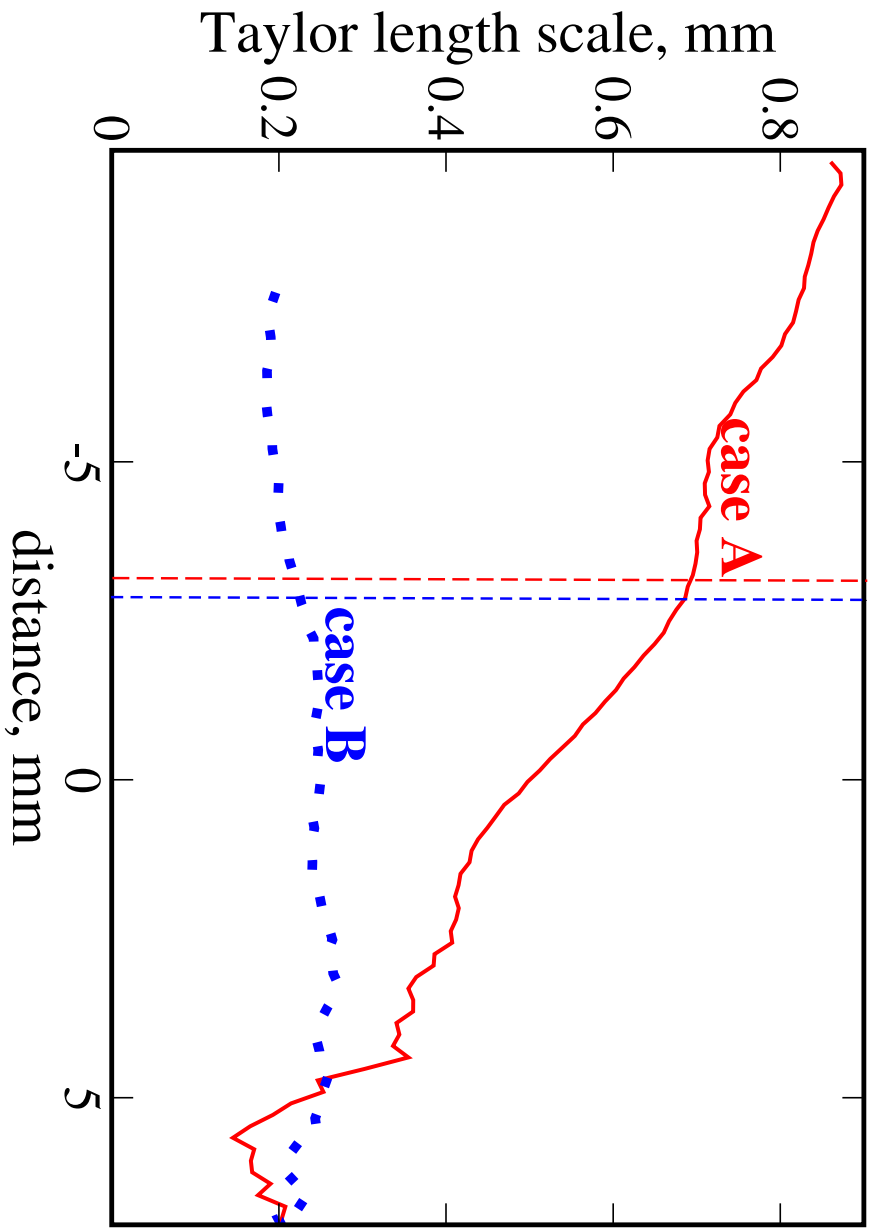

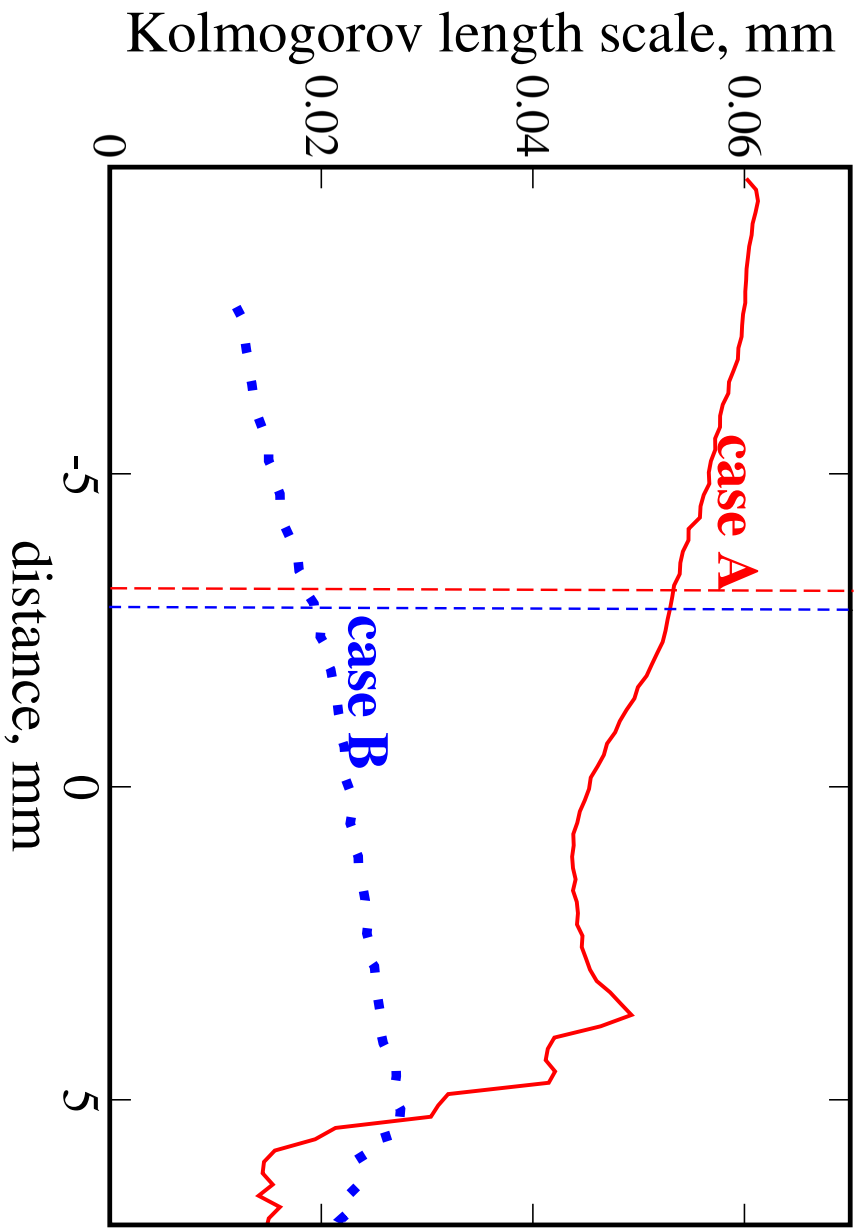

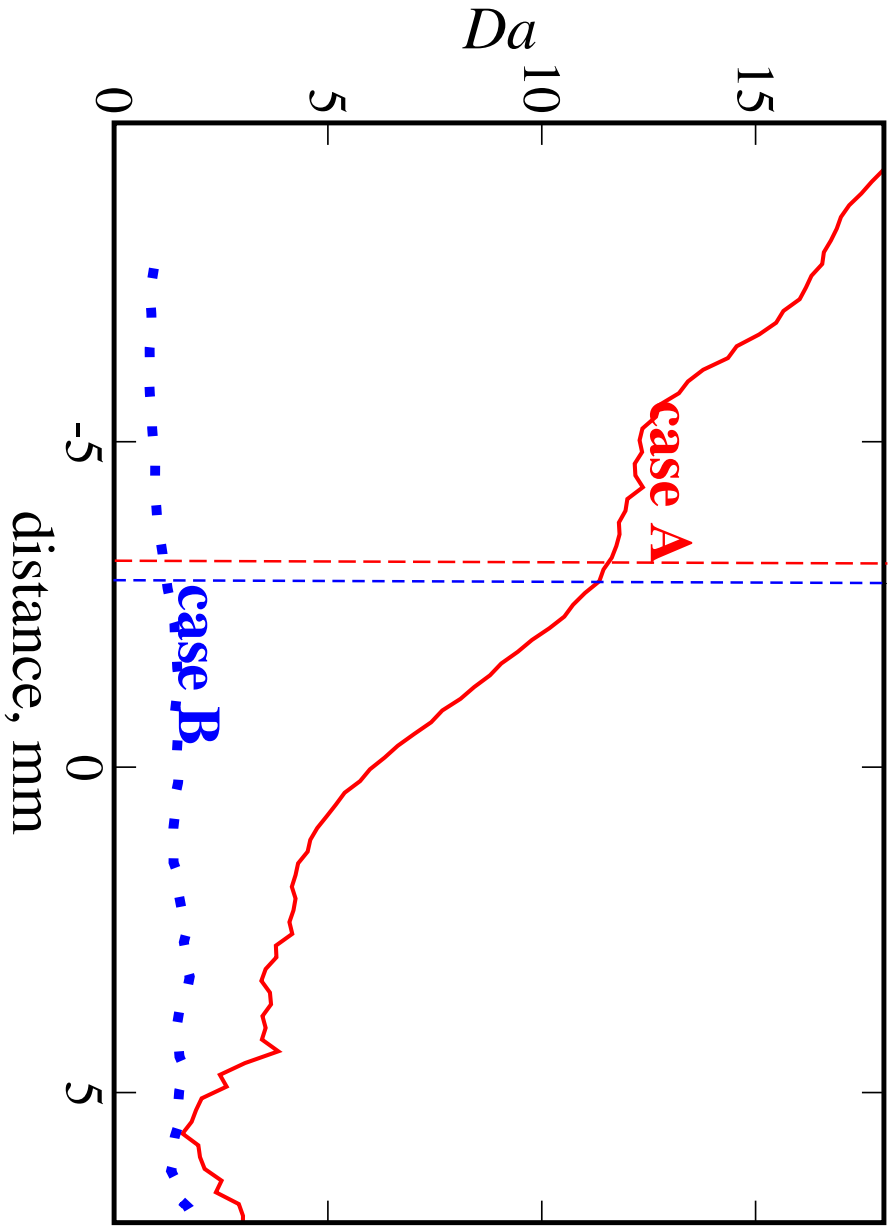

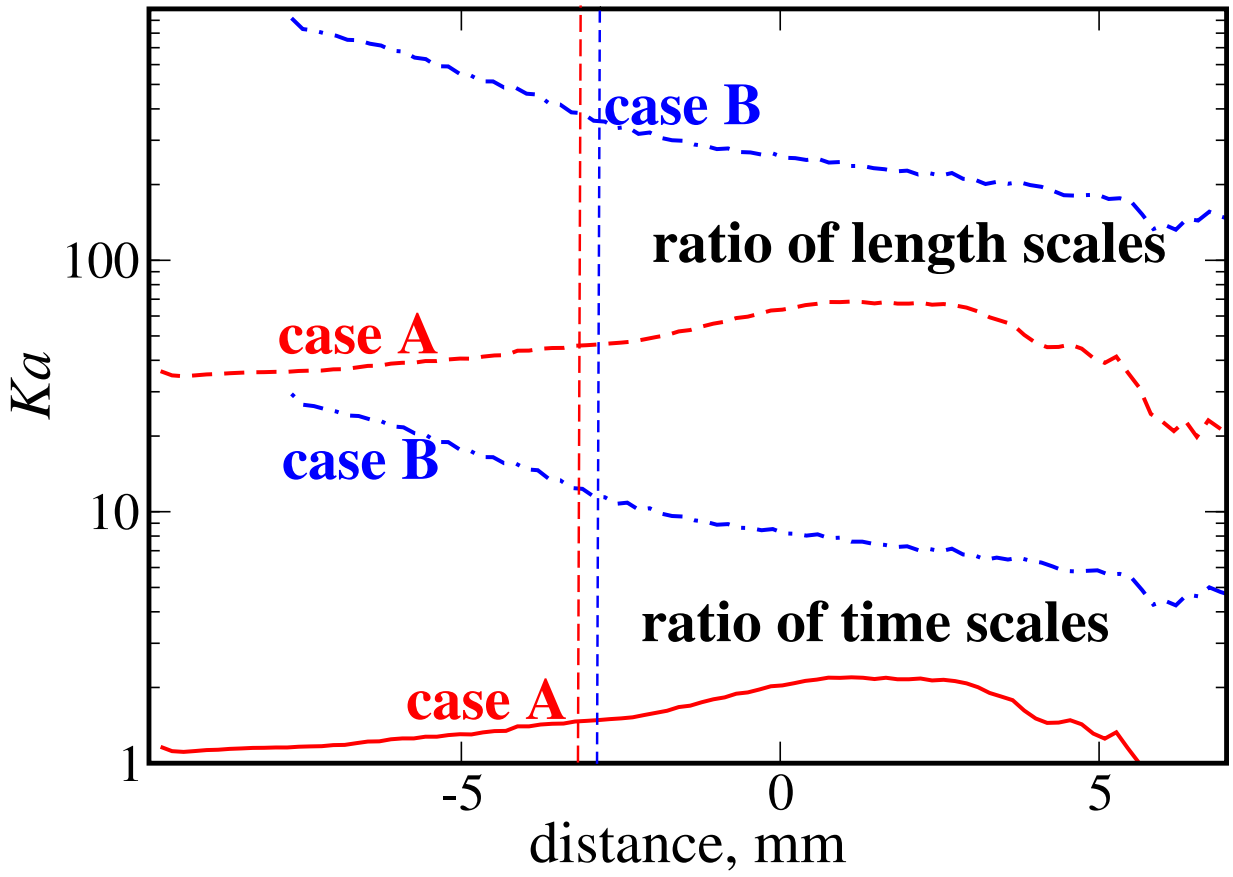

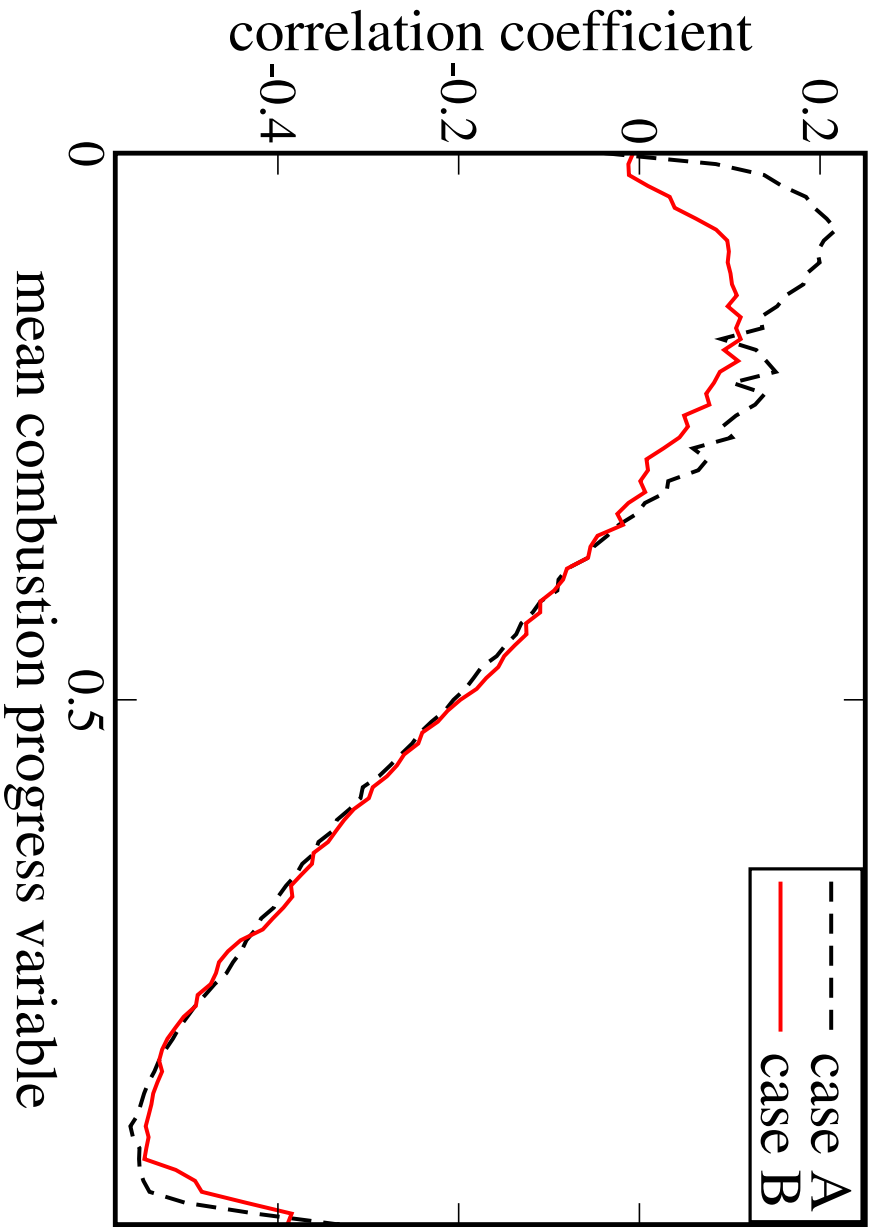

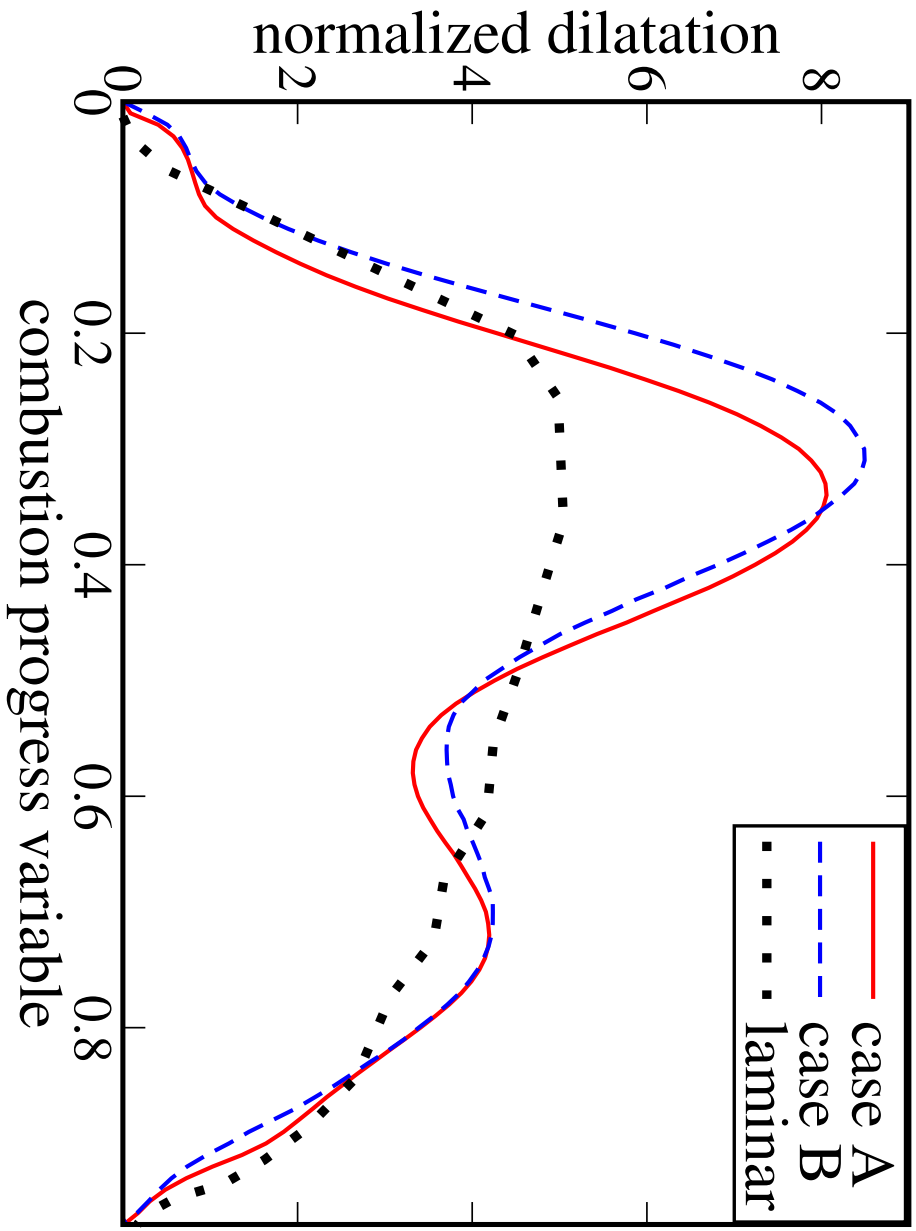

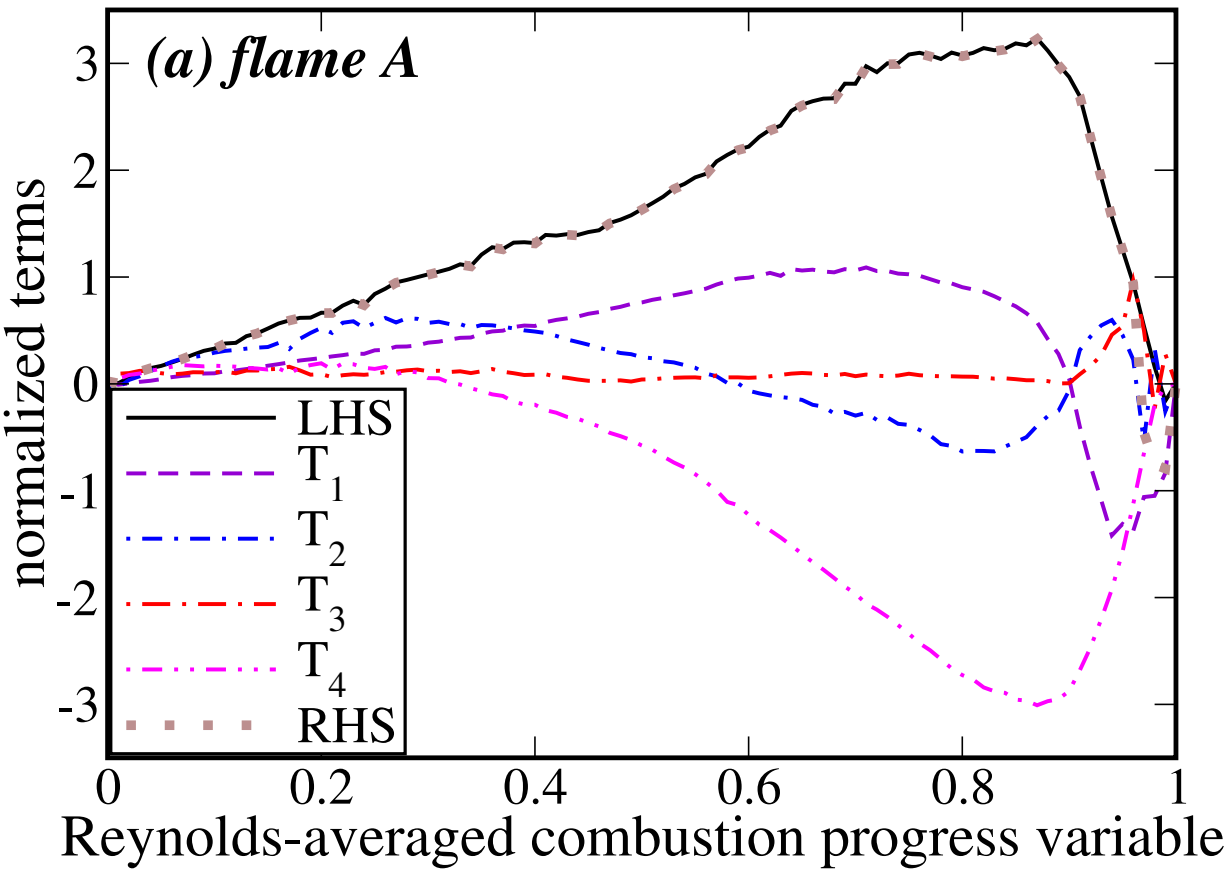

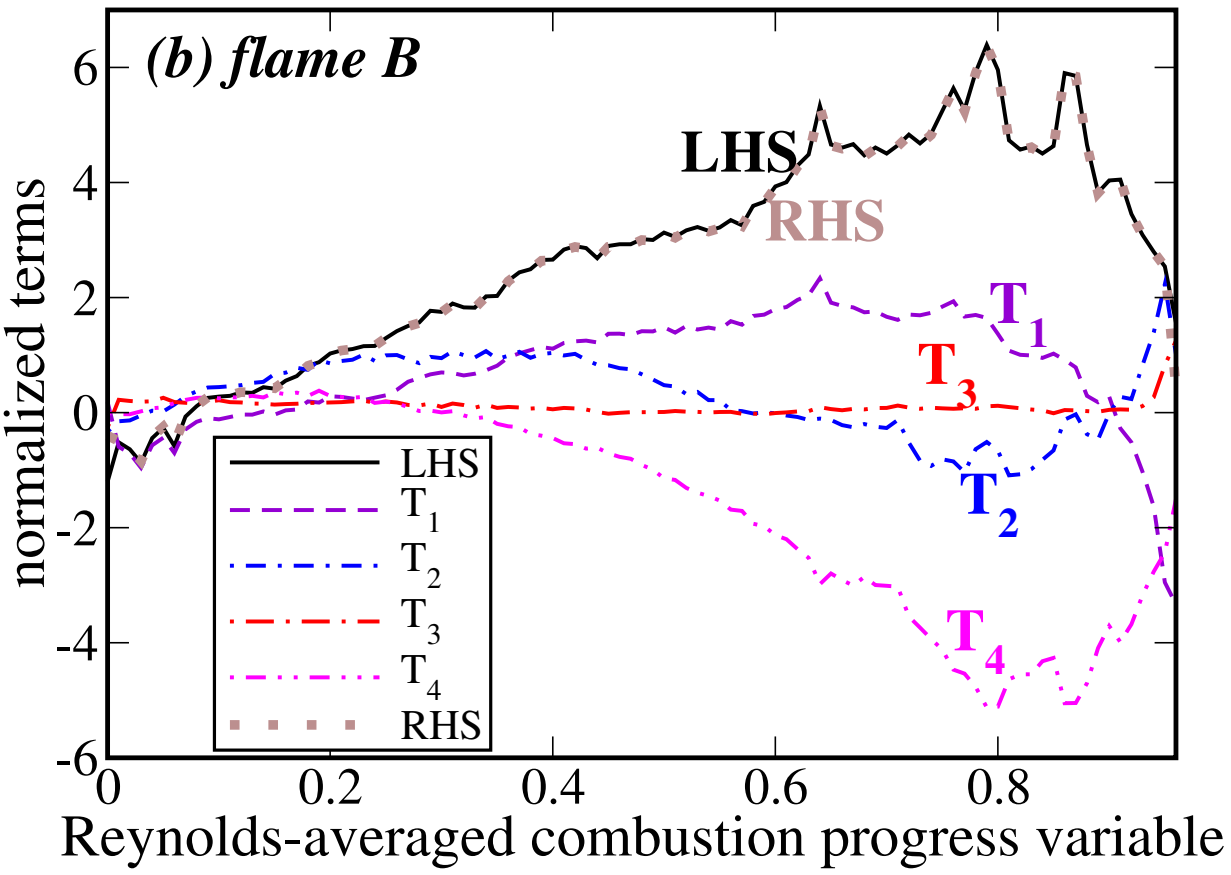

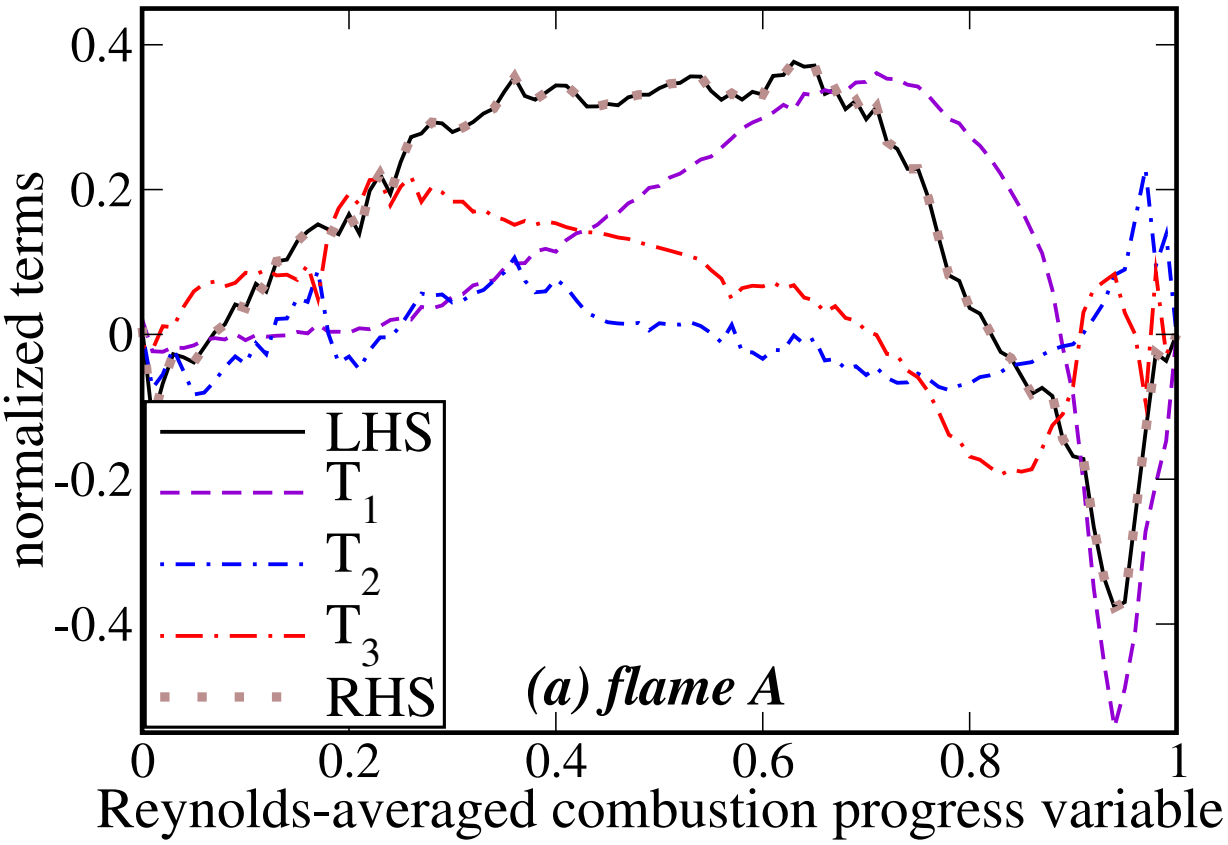

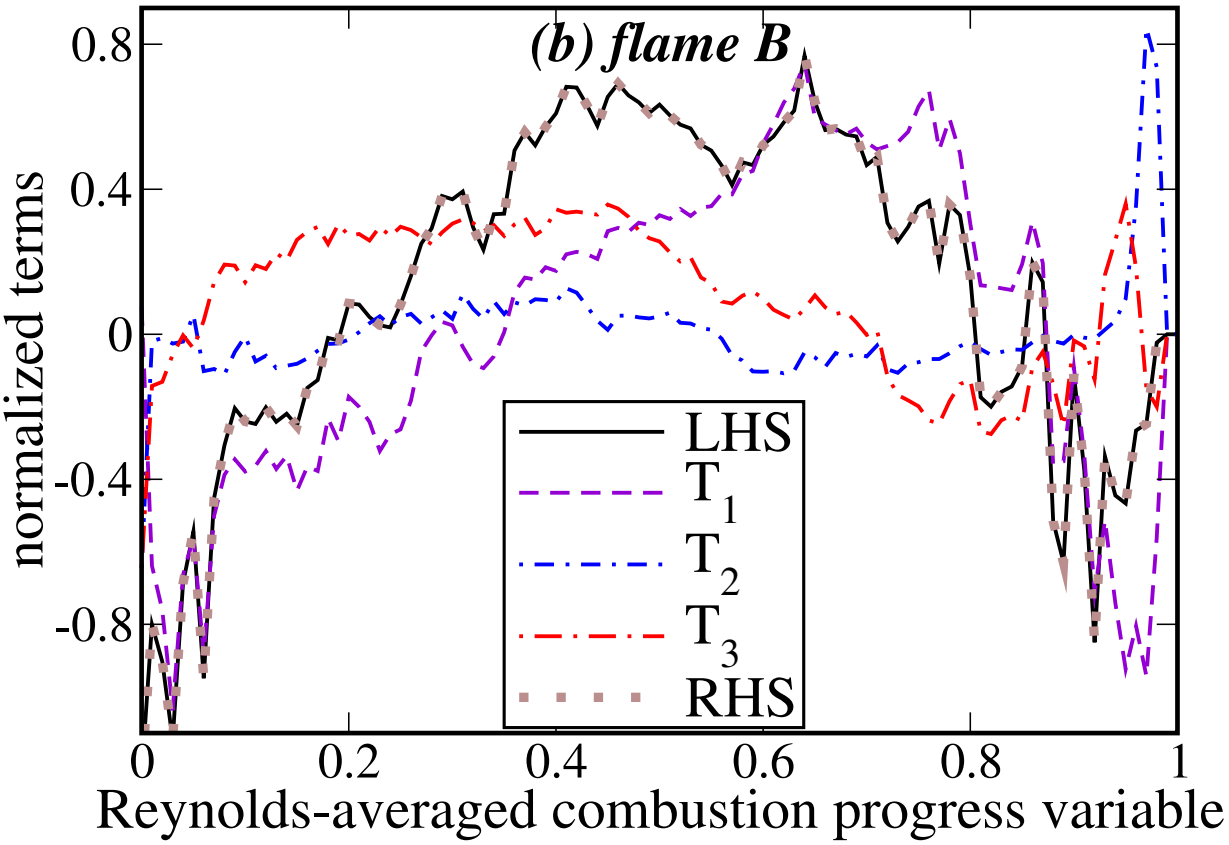

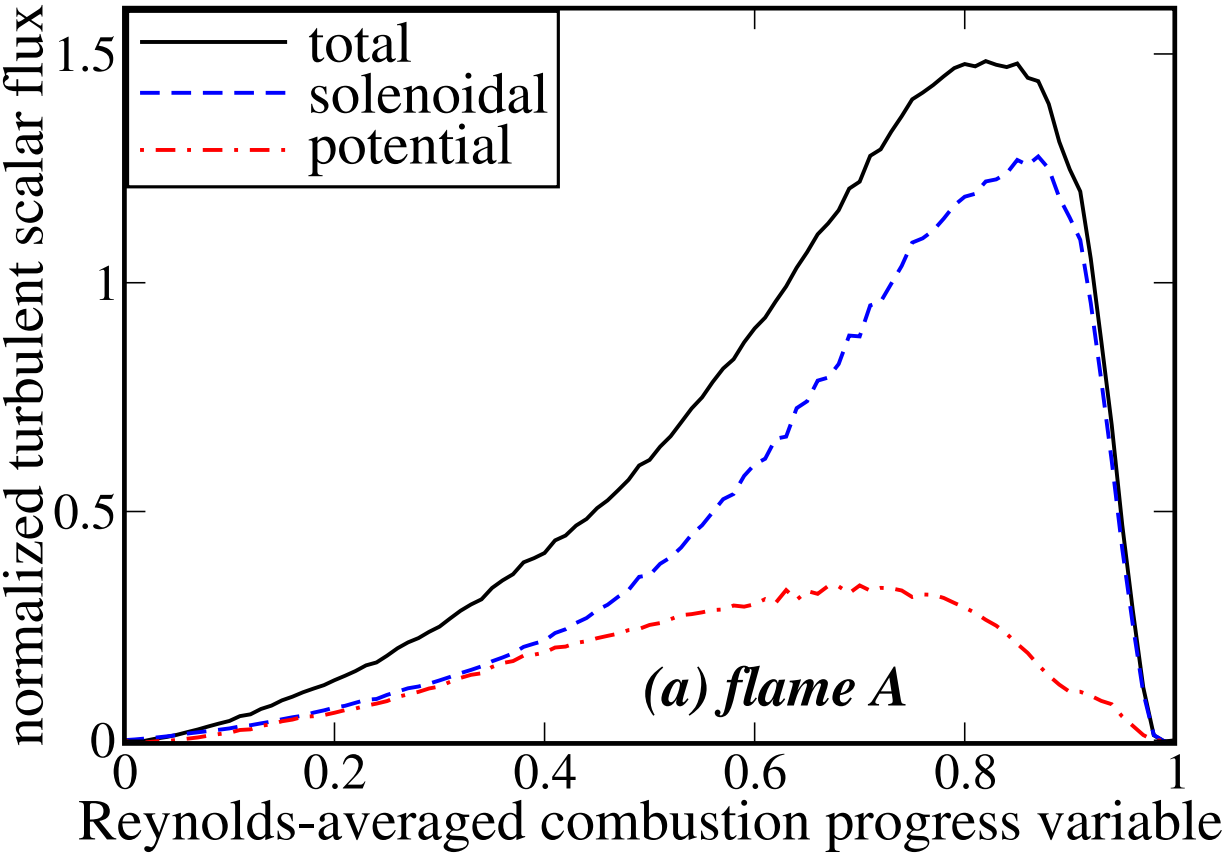

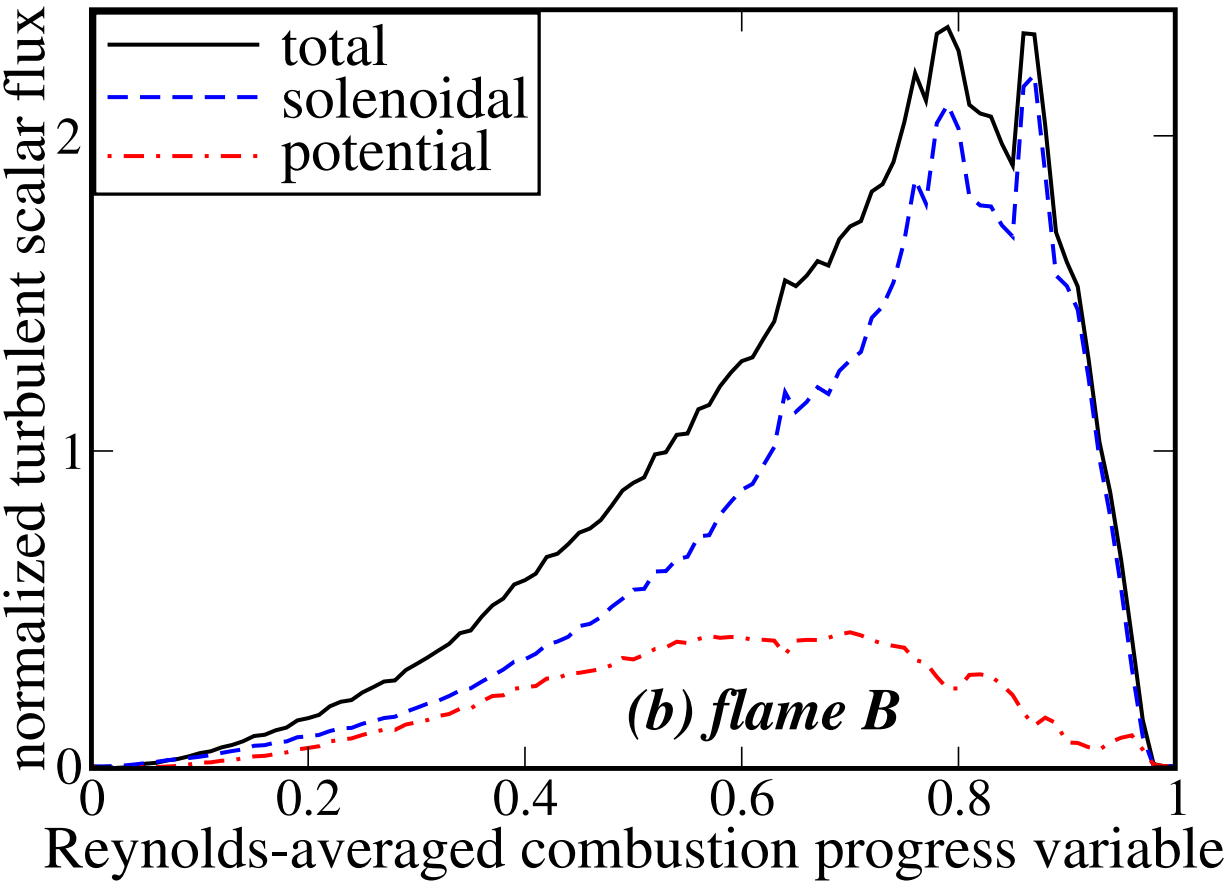

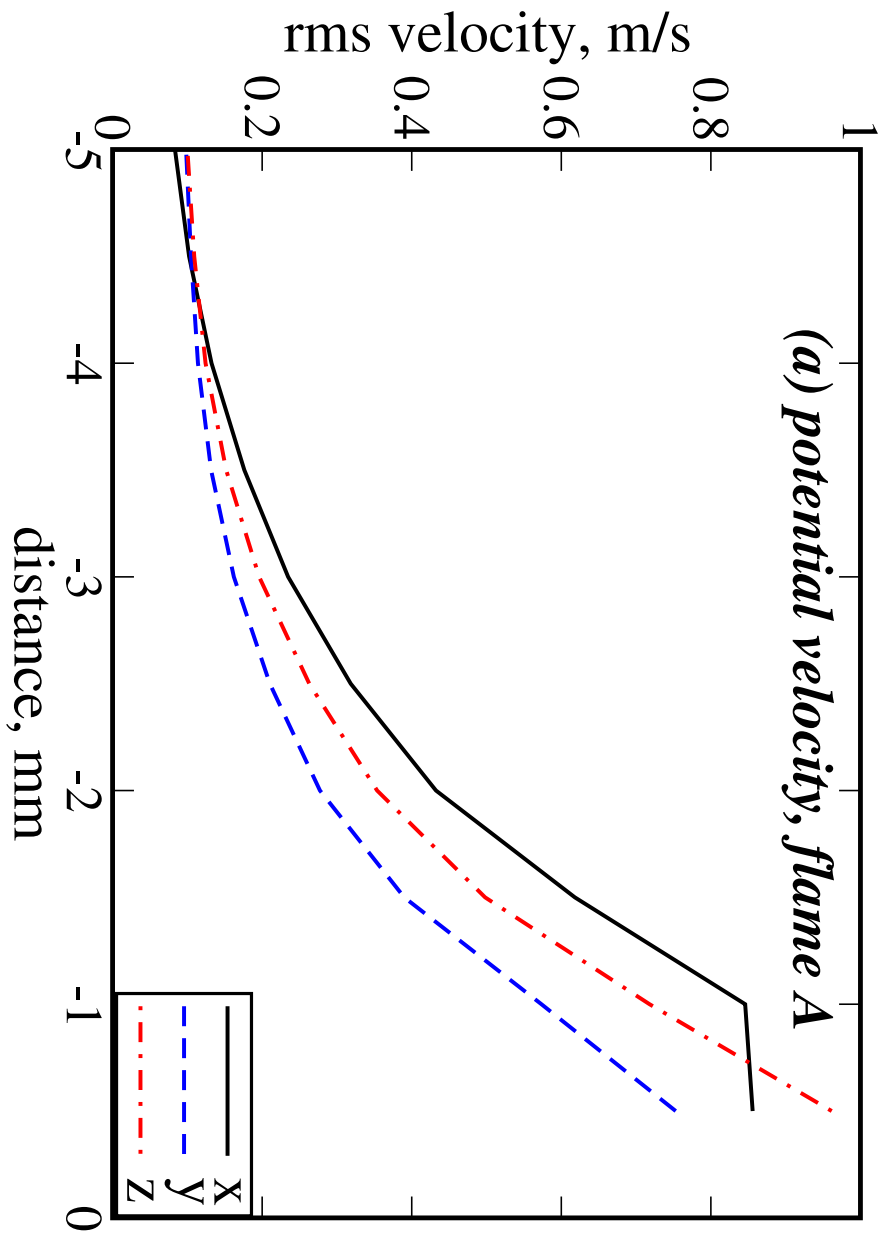

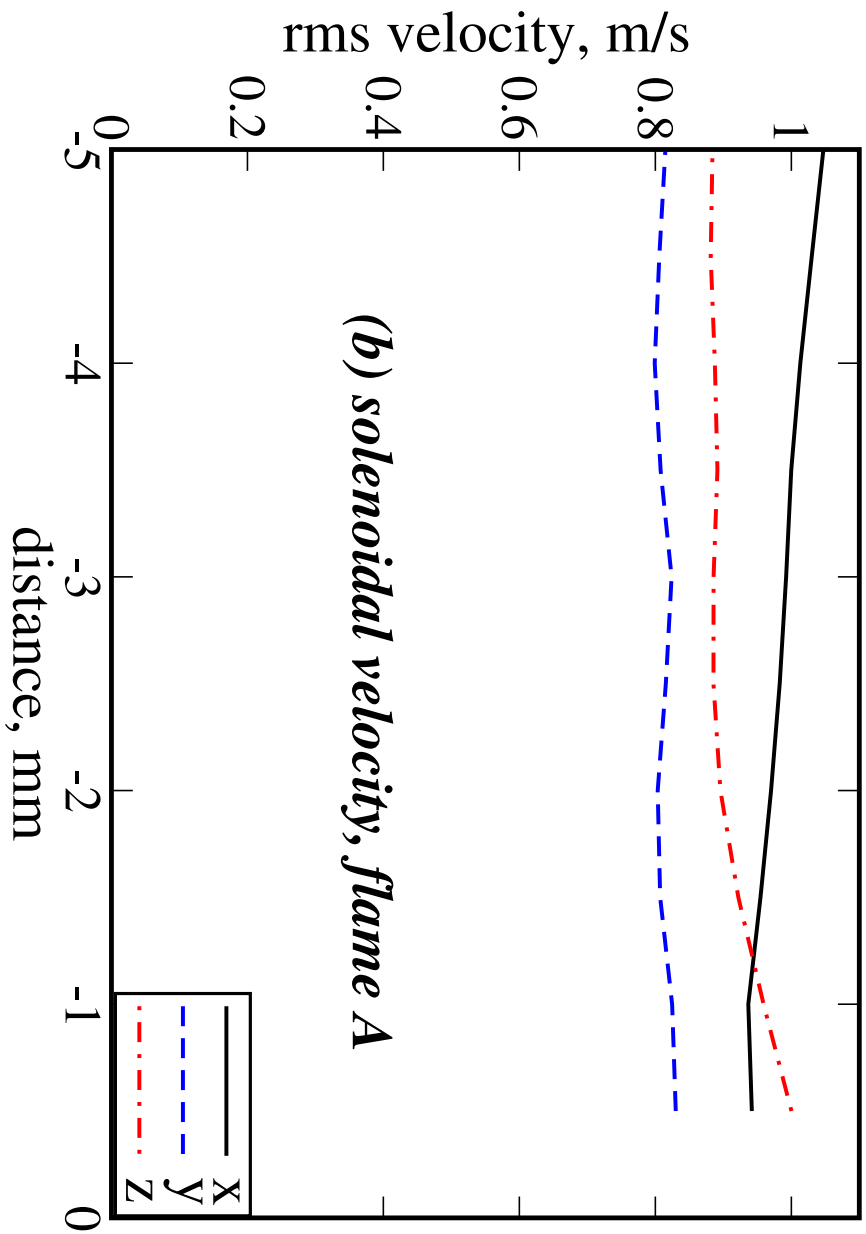

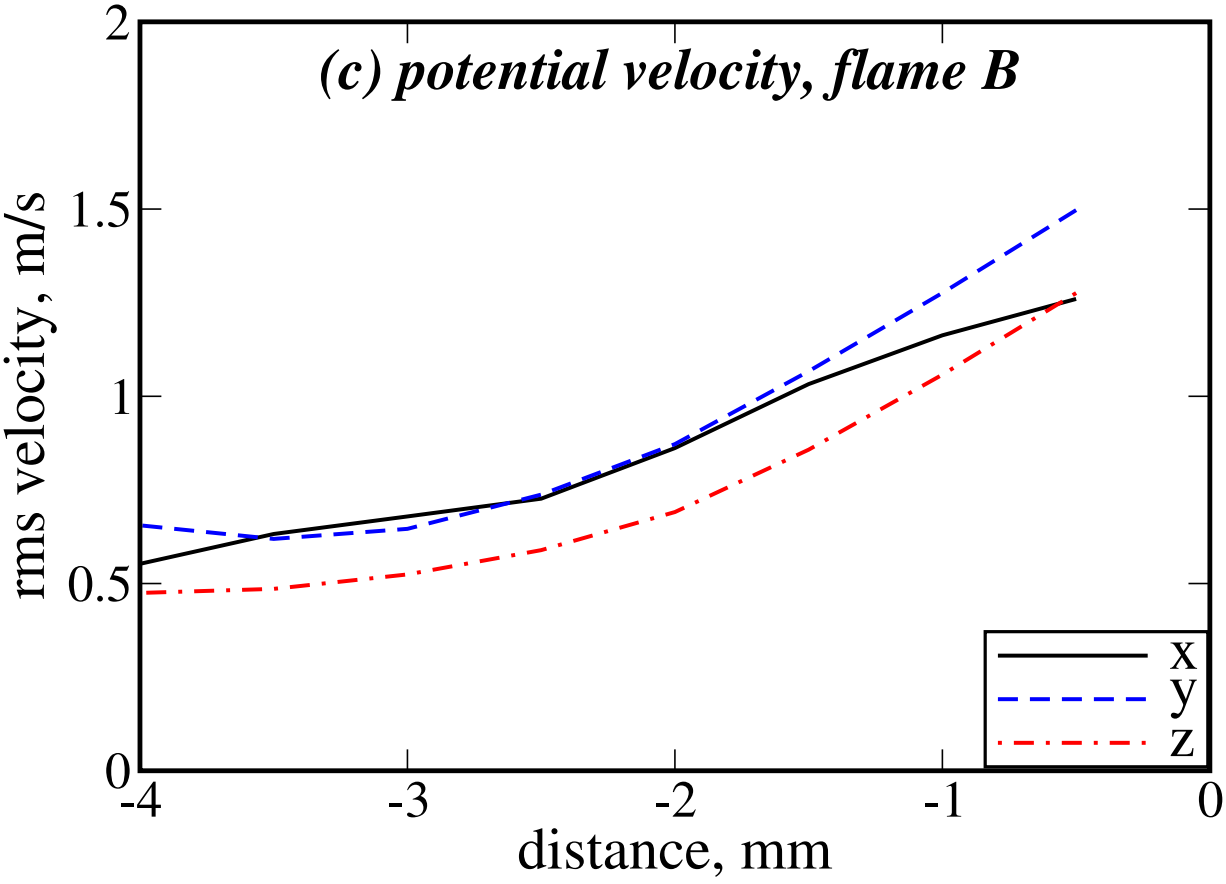

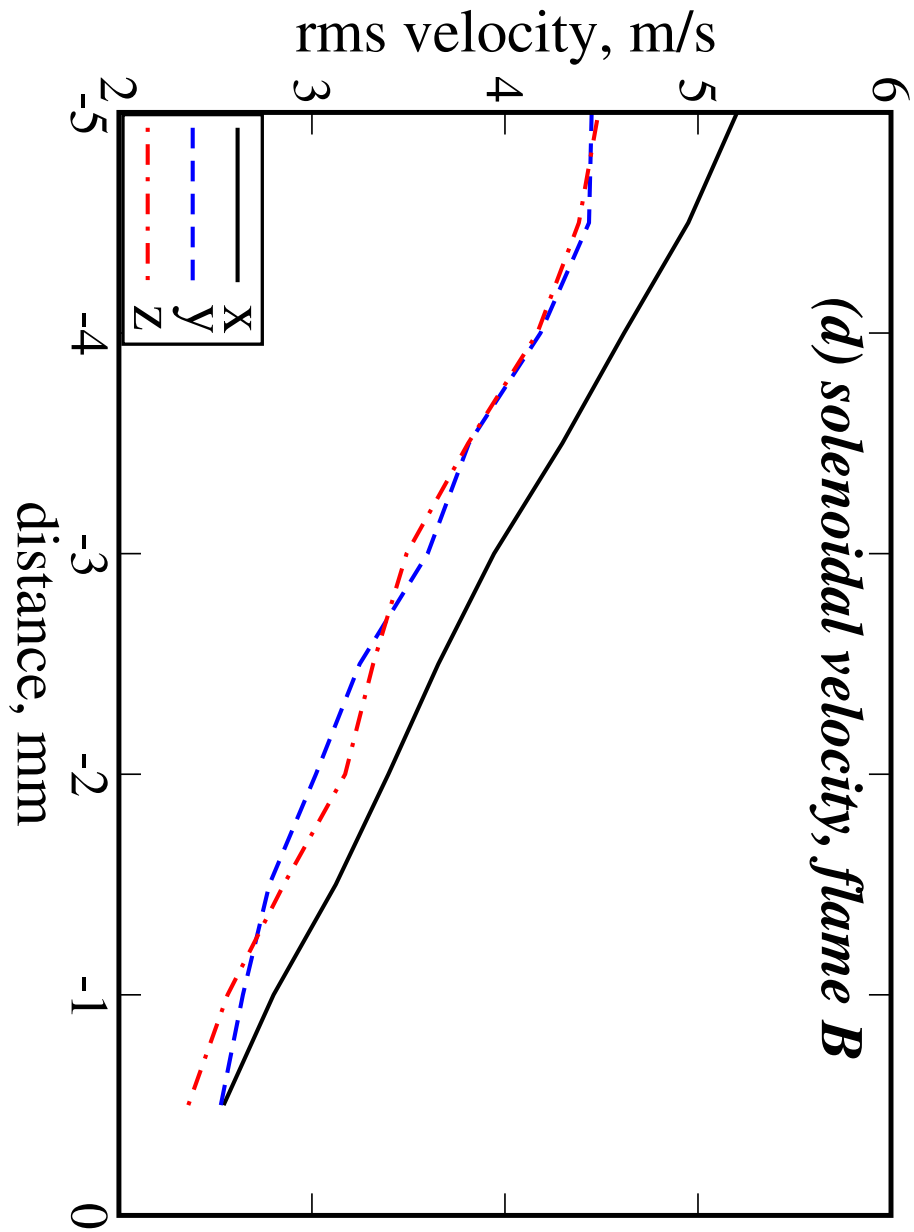

PLEASE CITE THIS ARTICLE AS DOI: 10.1063/5.0123211

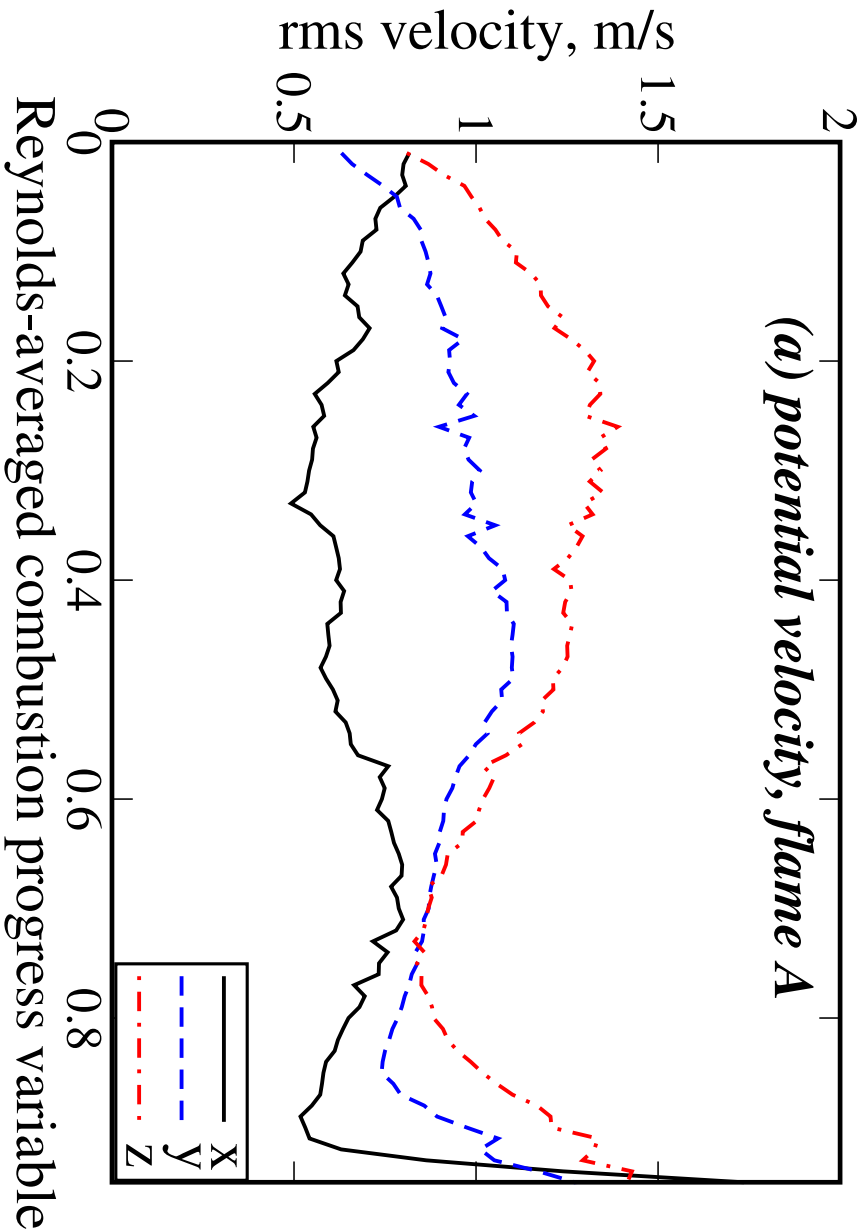

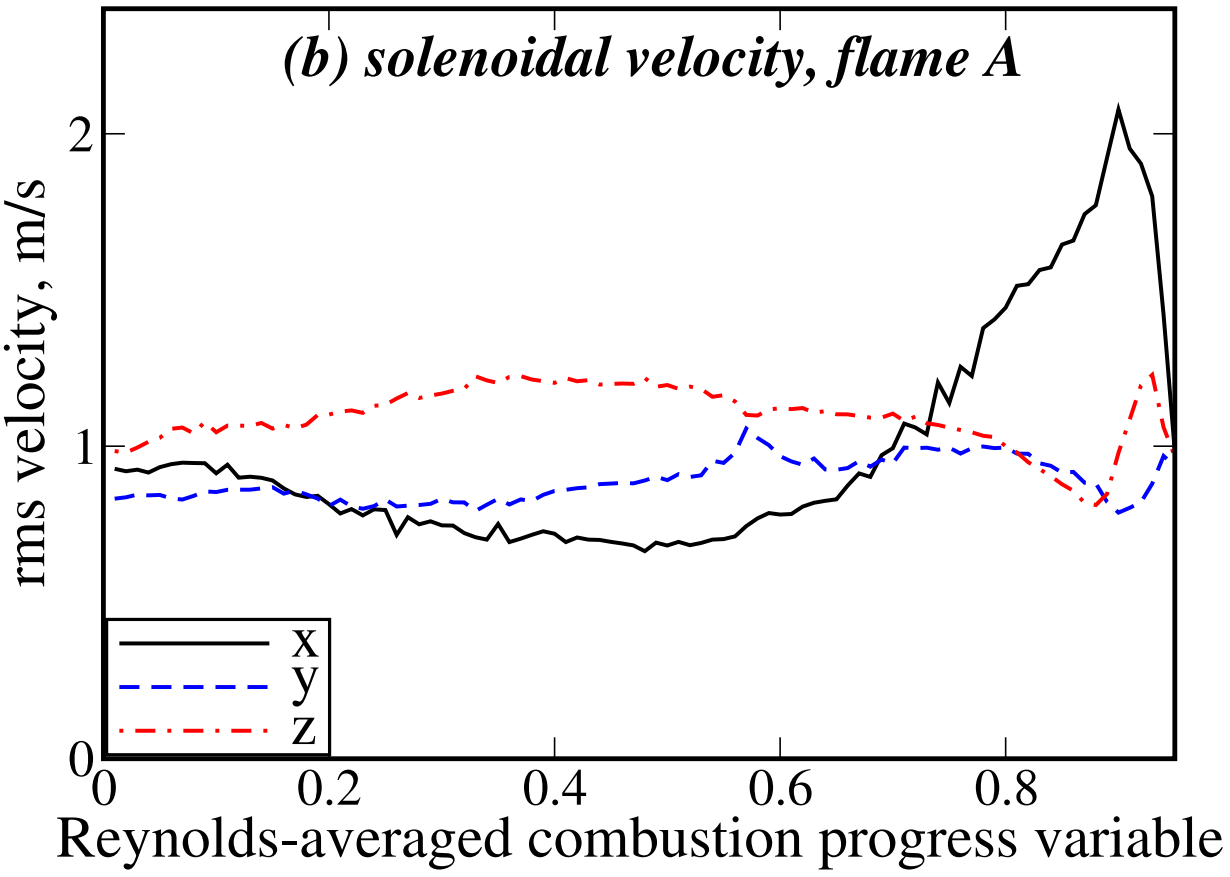

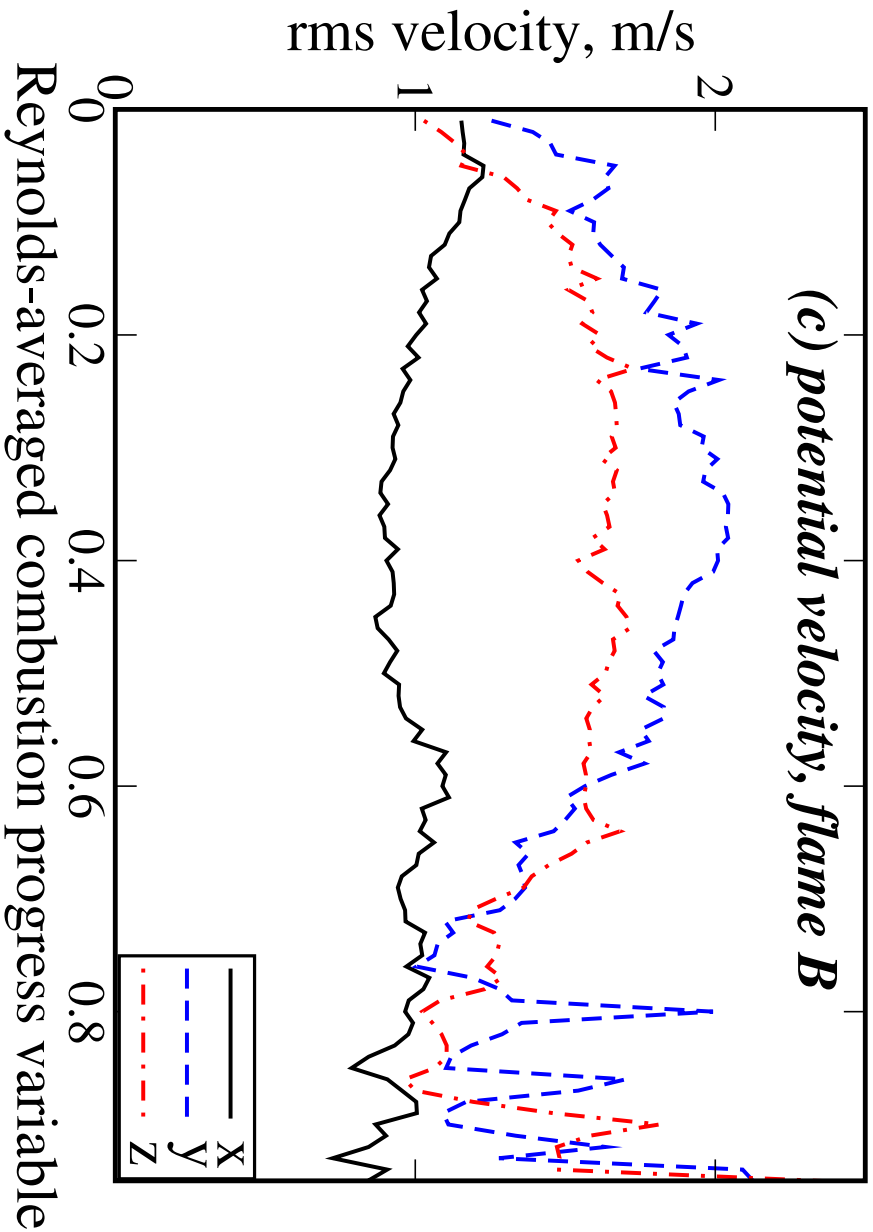

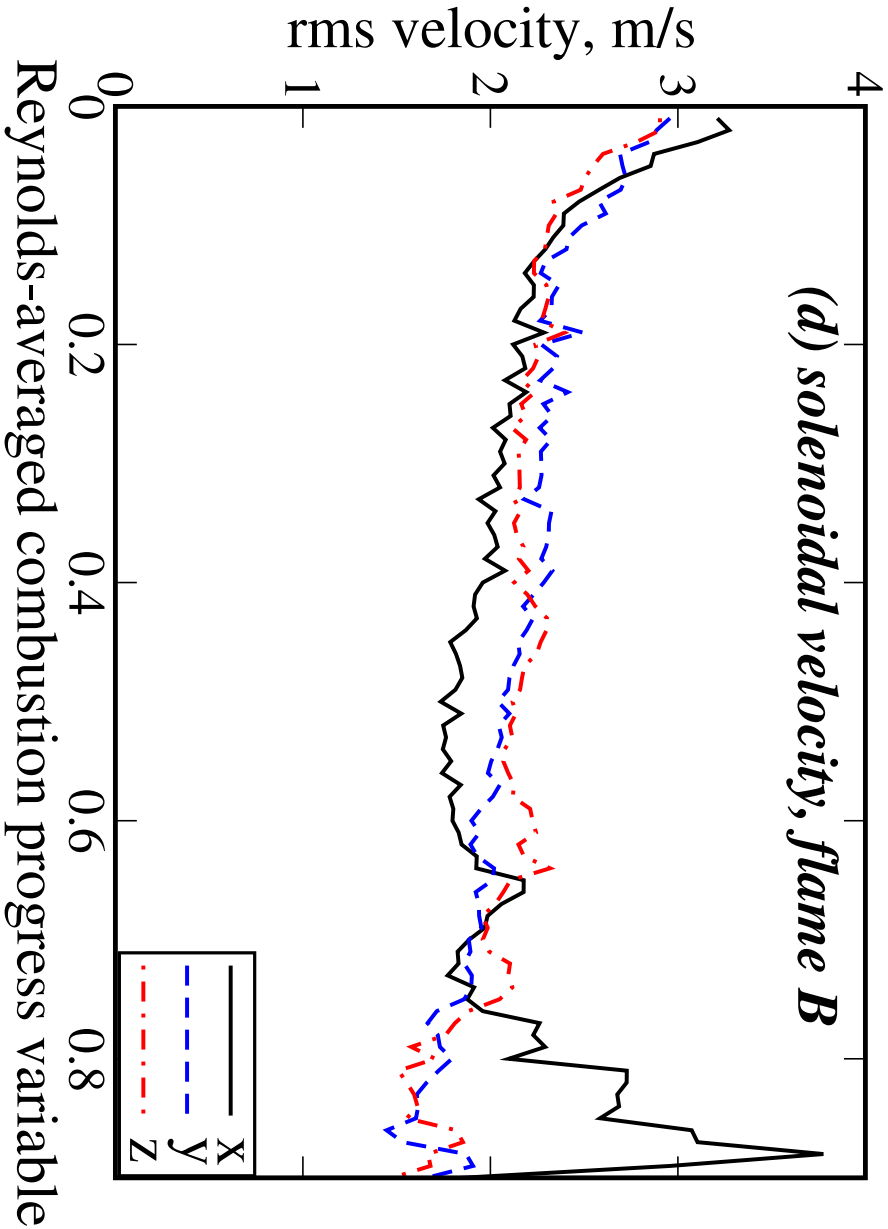

PLEASE CITE THIS ARTICLE AS DOI: 10.1063/5.0123211